修　士　論　文

Dumb Spatial Diversity Techniques in Industrial Wireless Communication

(産業用無線通信における
軽量型空間ダイバーシチに関する研究)

指導教員　　森川 博之 教授

東京大学大学院工学系研究科
電気系工学専攻

氏　　名　**37-155013**

Chutisemachai, Kulanuch
スティシーマーチャイ　グンラヌット

提 出 日　**2017 年 8 月 17 日**

Abstract

This thesis introduces dumb spatial diversity techniques for realizing industrial wireless communication, whose essential requirements are reliability and low latency. The open-loop spatial diversity techniques that are relatively capable for low latency are studied and adapted to be available for a massive number of transmitters, which is expected to provide the reliability over an entire factory. This thesis proposes massive simultaneous transmission and massive space-time block transmission.

Conventional simulcast requires tight carrier frequency control of every transmitter to ensure correct packet reception at a receiver, thus the careful transmitter selection is excessively complicated for implementation in a factory. Massive simultaneous transmission allows for greatly simpler transmitter deployment by exploiting the advantageous fast fading-like phenomenon resulted from the mismatched carrier frequencies to assist the demodulation, while the real-time capability is directly inherited from the simulcast.

Random generalization of unique signature vectors in distributed space-time block coding sacrifices real-time capability due to a demand of channel state information for demodulation. In addition, its distribution loss grows with the number of participating transmitters. Massive simultaneous space-time block transmission, on the other hands, deterministically assigns the codes to transmitters to reduce the distribution loss. A maximum-likelihood algorithm for demodulation where channel state information is not required is also applied to enable the low latency.

Contents

List of Figures

List of Tables

Chapter 1

Introduction

Wireless communication has been an attractive way to convey information for several decades. Its development is also known to be endless, as wireless communication has continuously been introduced to human's lifes for a long time: from telegraph, radio transmission, television, satellite, mobile communication, to short-range communication or wireless personal area. Industry section, as well, is also anticipating to fully welcome wireless technologies for data communication in the very near future.

This thesis explores wireless communication techniques for realizing industrial wireless communication.

1.1 Industrial wireless communication

In a factory, machines are commanded by control units to execute various tasks for industrial processes. Thus, data communication between the controllers and individual machine is considered as significant. An erroneous packet reception of a machine can lead to manufacturing malfunctions and fault production processes, which in turn ruins efficiency of production lines. Therefore, to prevent such a chain damage, accuracy in data communication between the controllers and machines is greatly expected.

Achieving the accuracy of industrial data communication implies that every machines precisely receive data packets within a determined period of time. Thus, the communication should be reliable and capable for rapid packet transmission and reception. Expectations on reliability and real-time capability of the industrial data communication are as follows:

- *Reliability*: Reliable data communication is crucial because not only accurate operation of machines can be ensured but quality of products are also guaranteed. The reliability of the data communication for industrial processes is generally measured in packet level. An allowed error rate depends on applications. For instance, industrial printing process allows for maximum error rate of 10^{-9} [8].
- *Real-time capability*: In order to preserve continuity of manufacturing processes, especially before and after occurrences of an occasional or emergency event, the data communication should be executed within a limited time, which is generally short. An end-to-end packet traveling time is expected to be within milliseconds. Similar to reliability, real-time capability also depends on applications. For example, industrial printing process allows for cycle time of 2 ms, while packaging process allows for more relaxed cycle time of 5 ms [1].

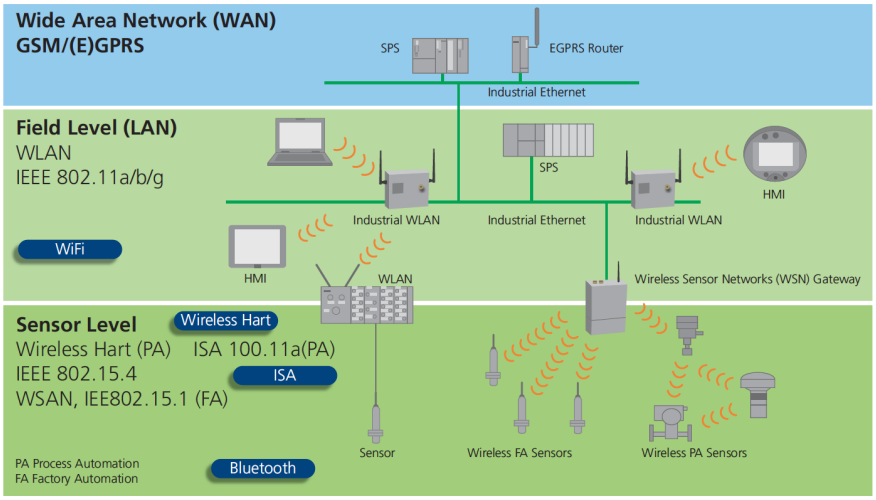

Fig. 1.1 An overview of industrial wireless communication [1].

Recent data communications in factories are mostly based on Industrial Ethernet (IE), such as EtherCAT and PROFINET IRT [9–12]. IE is a developed version of the high reliable Ethernet protocol, where its real-time capability is enhanced to suit the requirement of low latency. In addition, since cables are served as communication links between controllers and machines, IE systems also guarantee for the reliability.

Nevertheless, using wireless links to transfer data is apparently attractive when considering abilities of future industrial processes, where traditional manufacturings are going to be connected and integrated to realize flexibility, adaptability, efficiency, and increase effective data communication [13–16]. In a factory where a massive number of machines are placed, cables are mostly limited for achieving the targeted abilities. In contrast, replacing cables by wireless technologies allows for flexibility. Machines are able to move. Communication in an obstructed or shadowed areas, where cables are difficult for installation, is also operable. In addition, not only installation and maintenance cost of the cables, but network failure caused by fatigue, stress, and strain of the cables are also reduced.

Fig. 1.1 demonstrates an overview of industrial wireless communication. In order to achieve its requirements, some standardizations based on wireless sensor network (WSN) have been announced [17, 18]. For example, Wireless Interface for Sensors and Actuators (WISA) targets for wireless control [19]. WirelessHART [20], which is based on the HART communication protocol, targets for sensors and actuators, rotating equipment, and condition monitoring to address key end-user concerns such as reliability and specific purpose in industrial environment. ISA100.11a [21], which is developed by the International Society of Automation (ISA), targets for process automation and RFID to provide flexibility for

customizing the operation of a system. Nevertheless, the proposed standardizations trade off some reliability for low latency or vice versa.

1.1.1 Spatial diversity for reliability

Commonly, randomness of the wireless links makes wireless communication challenging. Particularly in a factory, where environment is harsh due to high heat; heavy dust; and plentiful metal obstacles, the links are more susceptible to attenuation and fading. Fortunately, the random links can be exploited to improve performance of the wireless systems, especially for the reliability, at a hand of diversity provided by independent fading paths.

The independent fading paths can be obtained by variously transmitting same information in different environments. Fig. 1.2 demonstrates overviews of diversity schemes: frequency diversity, time diversity, and spatial diversity. The same information transmitted on different frequency channels experience different fading condition, thus, frequency diversity can be exploited. To make the fading independent, carrier frequencies should be uncorrelated by separating at least a coherence bandwidth of the channel. Similarly, the same information transmitted at different time, where the interval is larger than a coherence time of the channel, provides time diversity. While frequency and time diversity can be exploited with a single transmitter and a single receiver, spatial diversity improves the performance by spatially placed several transmitters and/or receivers. Without a necessary to ensure the coherence bandwidth and time of the channel, signals from sufficiently separated transmitters experience uncorrelated attenuation and fading, where a receiver receives signals with various patterns for demodulation.

Because resources of the wireless communication, bandwidth, is limited, while the reliability and the capability for low latency are also essential for industrial wireless communication. Thus, among the diversity schemes, spatial diversity is applicable for the industrial wireless communication among the diversity schemes as deploying more transmitters and/or receivers does not conflict with the targeted expectations. Due to the limited bandwidth, exploiting frequency diversity by transmitting the information on different carrier frequency is wasteful. Besides, retransmission the information in different time is also struggle due to an increased latency.

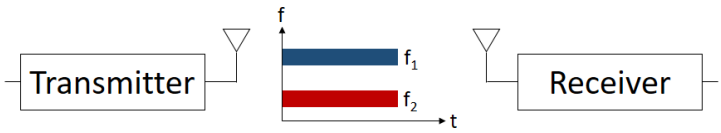

(a) Frequency diversity scheme.

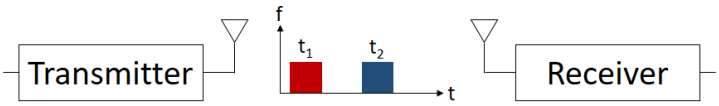

(b) Time diversity scheme.

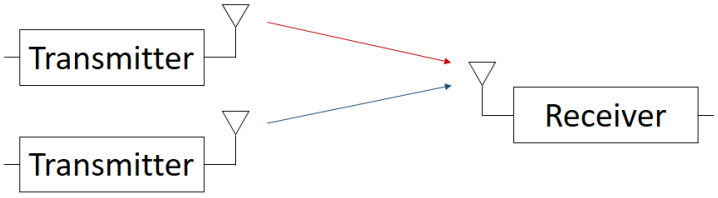

(c) Spatial diversity scheme.

Fig. 1.2 Overviews of diversity schemes.

1.1.2 Challenges for low latency

Conventionally, joint signal processing between multiple transmitters before data transmission is performed to further combat the randomness of the wireless links, i.e., cooperative communication. The cooperation allows transmitters to adapt their transmitting patterns to increase a probability of correct demodulation at a receiver. In order to efficiently assist the receiver, the transmitters perform the signal adaption according to channel status, which is given back by the receiver itself. This type of cooperative communication refers to close loop, since the receiver sends a channel state information back to the transmitters (CSIT), where the CSIT plays a key role for the reliability of the systems.

Fig. 1.3 illustrates a flow diagram of a transmitter selection scheme [22–28] as an example of the cooperative communication. The transmitters transmit pilot, or training, signals to the receiver in order to first inform the receiver the current channel status. After that, the receiver feeds the CSIT back, which is used to decide which transmitters will participate in data transmission. One or several transmitters that are likely to assist the demodulation of the receiver can be selected. It is obvious that even though transmission of pilot signals and selection process remarkably guarantee reliability, they also

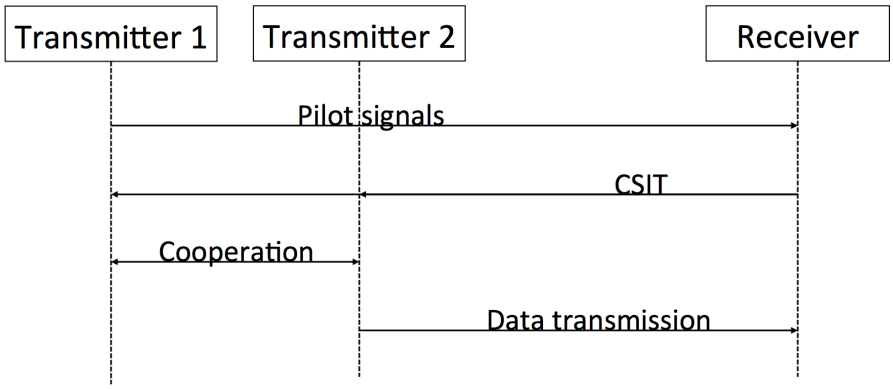

Fig. 1.3 A flow diagram of cooperative communication system.

induce substantial latency. In sum, the complex signal processing before data transmission prohibits a system to have the real-time capability.

Thus, to achieve stringent requirements of industrial wireless communication: reliability and real-time capability, this thesis *dumbs* conventional spatial diversity techniques to make them available for industrial wireless communication. Hence, massive simultaneous transmission and simultaneous space-time block transmission are proposed. Simulation of their performances, packet error rate (PER), on 2.45GHz-band IEEE 802.15.4 communication standard are performed under a real factory environment with various transmission-offset scenarios.

1.2 Thesis overview

This thesis contains five chapters. It is organized as follows:

Chapter 1: Introduction

This chapter introduces motivation and objective of the thesis. The thesis overview is also given.

Chapter 2: Open-loop techniques in distributed antenna system

This chapter studies open-loop spatial diversity techniques in distributed antenna system: simulcast and space-time block coding, which are likely to capable for low latency. The overview including fundamental knowledge of the techniques are also provided.

Chapter 3: Dumb spatial diversity techniques

To achieve the requirements of industrial wireless communication, this chapter proposes massive simultaneous transmission and simultaneous space-time block transmission. Side

effects from massive identical signals transmission are first discussed. The overview of the techniques including investigations on the transmission offsets, carrier frequency and timing offsets, are provided afterward.

Chapter 4: Evaluation

This chapter evaluates the performances of the dumb techniques on 2.45GHz IEEE 802.15.4 communication standard operating on 2.45GHz band under a real factory environment with various transmission-offset scenarios to investigate their feasibilities for industrial wireless communication. In addition, over-the-air experiments of massive simultaneous transmission are specially conducted to verify its feasibility in the real world.

Chapter 5: Conclusions and future works

This chapter concludes the contributions of this thesis as well as future improvements.

Chapter 2

Related works

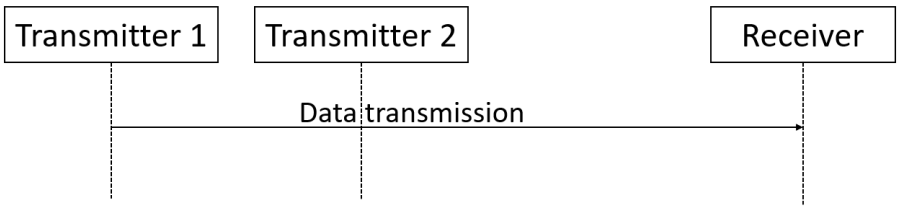

Fig. 2.1 A flow diagram of open-loop spatial diversity technique.

This chapter mentions related works of this thesis: open-loop spatial diversity techniques in distributed antenna system, in which the CSIT is not required. Thus, real-time capability of a system can be improved. The background of exploiting spatial diversity in the open-loop manner is first described. Overviews of the open-loop techniques: simulcast and space-time block coding, are provided afterward.

2.1 Open-loop distributed antenna system

A system in which its transmitters transmit information without paying attention to channel status, in other words, CSIT is unnecessary, refers to an open-loop system [29]. Compared to a close-loop system, the open-loop one induces less complexity because cooperation level between transmitters is lower, as illustrated in Fig. 2.1

Achieving the spatial diversity by the open-loop manner can be accomplished by multiple antenna system and distributed antenna system. Massive antenna system focuses on an individual transmitter and/or receiver that is equipped with multiple antennas, as demonstrated in Fig. 2.2. Massive antenna system is well known for multiple-input multiple-output (MIMO) systems. To efficiently provide the spatial diversity, the antennas should appropriately be separated in order to create highly independent fading paths [30].

Focusing on transmitter side, a concept of distributed antenna system including comparison of its coverage with single antenna system are illustrated in Fig. 2.3. Distributed antenna system splits a single transmitter into multiple, where they are ubiquitously placed over an area in order to provide everywhere-accessible wireless communication, for example, in a large building. Thus, connection links between transmitters and any receiver can be ensured since a probability of the receiver to be able to communicate with at least one transmitter in a shadowed or obstructed area is increased [31, 32]. In contrast to massive antenna system, whose limitation is coverage, distributed antenna system not only expands the coverage but each transmitter can also be equipped with multiple antennas to improve the reliability of the system, note that with an expense of complexity.

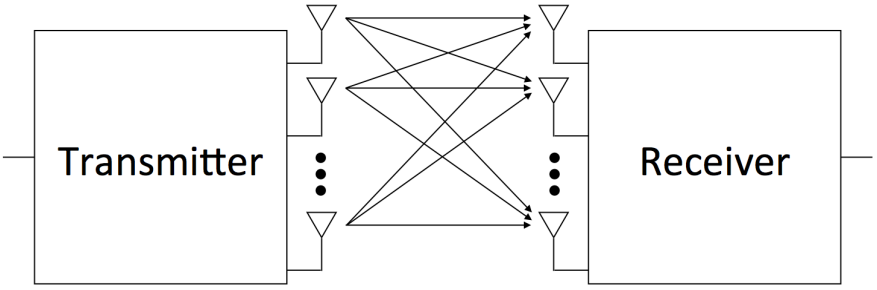

Fig. 2.2 Multiple antenna system.

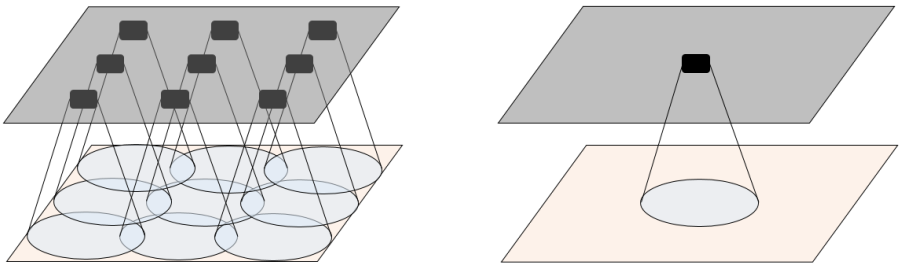

(a) Distributed antenna system. (b) Single antenna system.

Fig. 2.3 Coverage of distributed and single antenna system.

Since distributed antenna system gains advantages over multiple antenna system in the coverage aspect, it is more suitable for a factory, where the area is in an order of several square meters. In the later sections, open-loop spatial diversity techniques: simulcast and space-time block coding, which are applicable in distributed antenna system, are revealed.

2.2 Simulcast

Simultaneous broadcast of same information from multiple transmitters on a single carrier frequency refers to simulcast. According to the simultaneous transmission, one of advantages of simulcast is that signal processing before the transmission is very simple. The transmitters do not require any cooperation except timing synchronization. Thus, simulcast systems are naturally capable for low latency. The use of simulcast in wireless communication systems can be dated back to 1970s, in an early era of mobile communication. Currently, simulcast is still being used, especially in WSN area [4, 33–37], in which it is known as concurrent transmission. The concept of simulcast is shown in Fig. 2.4, where the simultaneous transmitted signals are expected to combine in a way that it assists demodulation at a receiver, i.e., constructive interferences occur.

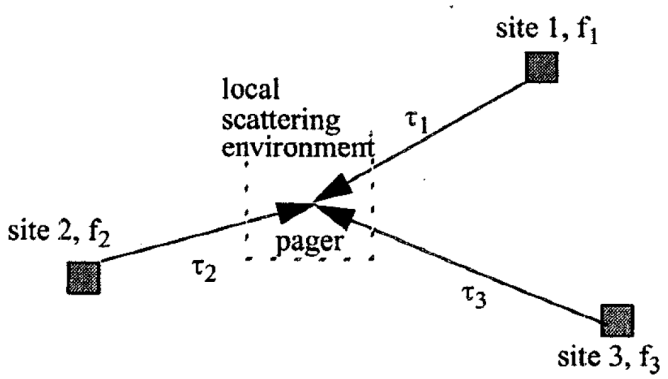

Fig. 2.4 An overview of simulcast in paging system [2].

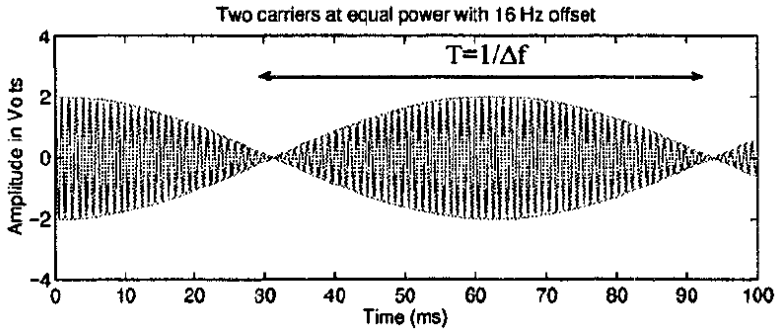

Fig. 2.5 Beating pattern in time domain [2].

Nevertheless, besides the constructive interferences, the combination of the signals can result in destructive, which does not help the receive to achieve correct demodulation The destructive signal superposition occurs in form of beating and intersymbol interference (ISI). Beats, as shown in Fig 2.5, are caused by phase cancellation of the transmitted identical signals with synchronized time but slightly different carrier frequencies. Analysis on effects of the beating mostly have been conducted in the early era of mobile communication [2, 38–40], where cancellation points, or nulls, occur periodically at the offset frequency. In other words, period of the beats is a reciprocal of a difference of exact carrier frequency each transmitter uses to transmit the identical signals. Hence, beating period T_b can be expressed as

$$T_b = \frac{1}{\Delta f}, \tag{2.1}$$

where Δf represents the offset frequency.

At a null point, signal amplitude severely drops. As a result, the receiver might not be able to demodulate the signal if its signal-to-noise ratio (SNR) is insufficient.

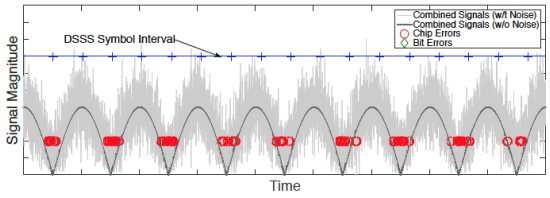

(a) Beating effect with large Δf.

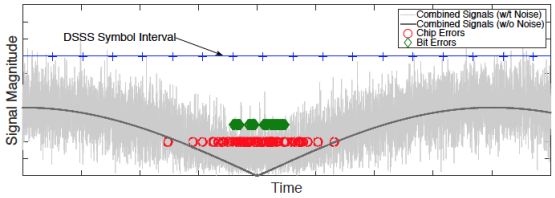

(b) Beating effect with small Δf.

Fig. 2.6 Erroneous chips caused by offset frequencies [3].

Examples of the beating problem on the performance of mobile communication are discussed in [2,39], where a paging system called FLEX was analyzed. A transmitted data of FLEX system operating on 900MHz band at 6,400 bps can be seen as a 32×32 matrix consisting of BCH(32,31) codewords, where a codeword contains 32 bits. A transmission order, however, is in column wise. That is the first bits of every codeword are transmitted first, then the entire second bits and so on. A duration for transmitting 32 bits equals to 5 ms. If the Δf equals to 200 Hz, which results in $T_b = 5$ ms, the null points occur at every bits of a codeword. Consequently, the receiver fails to correctly demodulate the erroneous codeword, which in turn causes an erroneous reception.

To spread the errors over several bits of several codewords, the carrier frequencies of transmitters, or base stations, in the paging systems are set according to a certain offset allocation. In [39], recommended certain offset frequencies are {-45, -30, -15, 0, 15, 30, 45} Hz for the 900MHz band FLEX 6,400 bps system. By certainly set the offset, not only reliability can be improved, the coverage area of the system also is expanded.

Recently, study in [3] has analyzed the beating problem in WSN. According to the characteristics of sensor nodes, where oscillators of radio modules are not consistent, certainly set the offset frequencies is difficult. Nevertheless, since T_b occurs periodically at a rate of a reciprocal of the offset, making it smaller than a symbol period can ensure successful packet reception because the errors occurring in a symbol level hardly affect sequences of data bits. Therefore, the offset frequencies might not be tightly controlled, but should

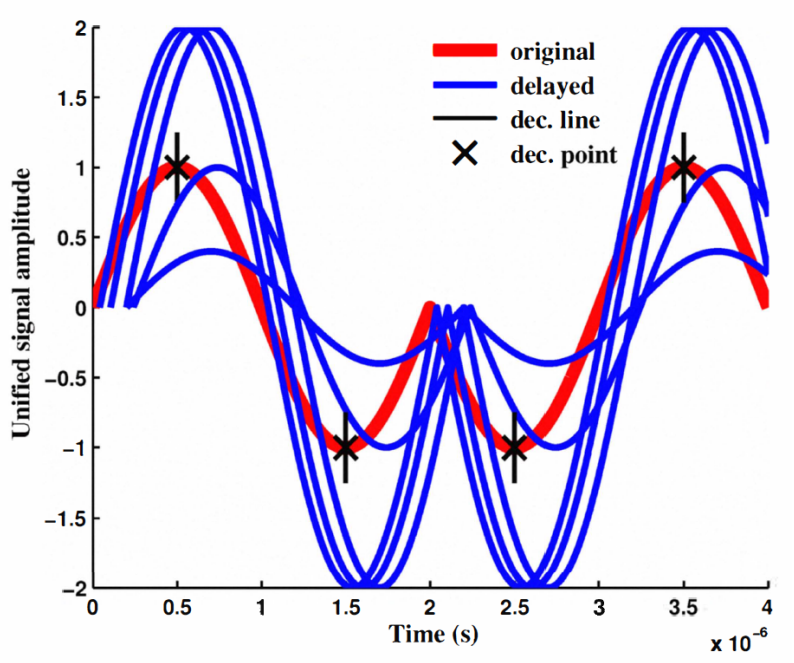

(a) Delayed signals arriving within a threshold.

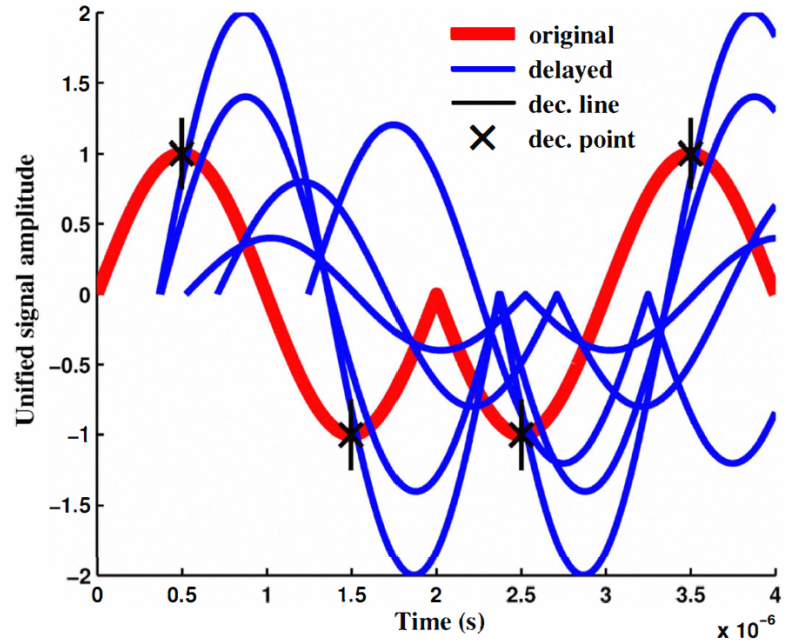

(b) Delayed signals arriving later than a threshold.

Fig. 2.7 Delayed signals [4].

be ensured to be sufficiently large in order to create small beating period. The effect of beating on a direct sequence spread spectrum (DSSS) symbol are shown in Fig. 2.6.

Another criteria that successful simulcast in WSN depends on is a severity of ISI. The simultaneous transmitted signals may arrive at a receiver with different time, which can be caused by, for example, different distance between the transmitter and the receiver. Fig. 2.7 demonstrates the replicas of delayed signal, where the receiver cannot make a precise decision if the delayed signal arrive later than a threshold. [4, 34] have suggested a limited time delay should be achieved so that the occurred ISI can be negligible and does not effect the performance of the demodulation. Particularly, [34] has conducted an on-chip experiment of IEEE 802.15.4 standard compliant WSN. The work has suggested to control the timing difference of consecutive signals to be within 0.5 μs, or a chip period T_c [41], in order to ensure constructive interferences and, thus, successful reception.

2.3 Space-time block coding

Space-time block coding (STBC) provides the spatial diversity by separately transmitting an encoded symbols on multiple transmit antennas. The transmitted symbols are orthogonal, that is the symbols are complex linear combinations of themselves and their complex conjugates.

The concept of STBC was first proposed by Alamouti [42] as a simpler space-time coding scheme according to a use of maximum likelihood algorithm (ML) for demodulation. The Alamouti scheme is designed for two transmit antennas, where a sequence of symbols, $s = \{s_1, s_2\}$, are encoded and splitted to each transmit antenna for simultaneous transmission as demonstrated in Fig. 2.8. In the Alamouti scheme, a matrix of transmitted symbols can be expressed by

$$\mathbf{S} = \begin{bmatrix} s_1 & -{s_2}^* \\ s_2 & {s_1}^* \end{bmatrix}, \tag{2.2}$$

where ${s_1}^*$ and ${s_2}^*$ are complex conjugate of symbols s_1 and s_2, respectively. At time t, transmit antenna one and two simultaneously transmit s_1 and s_2, respectively. At time $t + T$, T is a symbol period, transmit antenna one and two simultaneously transmit $-{s_2}^*$ and ${s_1}^*$, respectively.

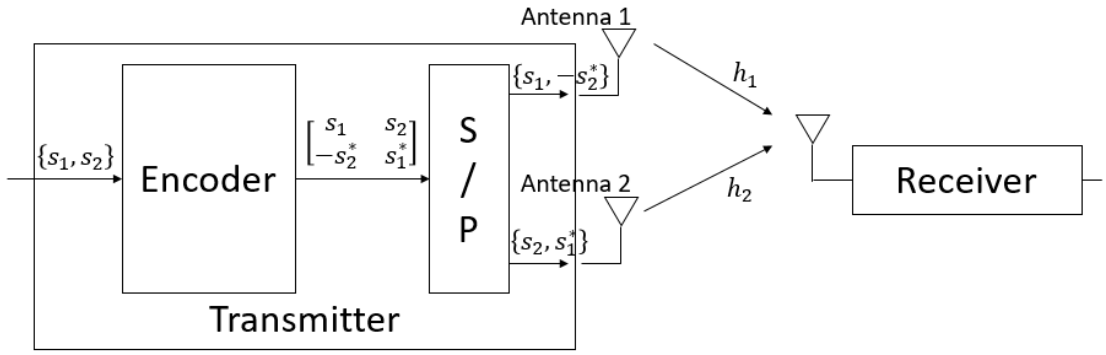

Fig. 2.8 The Alamouti scheme with one receive antenna.

At a receiver, for simplicity is assumed to be equipped with one receive antenna, two transmitted symbols affected by different fading and noise combine. Therefore, received signals at time t and $t+T$ are

$$\begin{aligned} r(t) &= h_1 s_1 + h_2 s_2 + n(t) \\ r(t+T) &= -h_1 {s_2}^* + h_2 {s_1}^* + n(t+T), \end{aligned} \tag{2.3}$$

or can be expressed in a matrix form of,

$$\mathbf{R} = \mathbf{HS} + \mathbf{N}. \tag{2.4}$$

$\mathbf{R} = \left[r(t)\ r(t+T) \right]^{\mathrm{T}}$ is a matrix of received symbols. $\mathbf{H} = \left[h_1\ h_2 \right]$ is a matrix of channel coefficients between the two transmitters and the receiver, where h_1 and h_2 are assumed to be quasi-static, or static over a data packet. $\mathbf{N} = \left[n(t)\ n(t+T) \right]^{\mathrm{T}}$ is a matrix of zero-mean complex Gaussian random noise. $[\cdot]^{\mathrm{T}}$ denotes transposition of a matrix.

From Equation 2.3, to extract received symbols $\hat{s} = \{\hat{s_1}, \hat{s_2}\}$ from $\mathbf{R}$, h_1 and h_2 should be disappeared, which is achieved by the property of the complex conjugate, that is

$$\begin{aligned} \hat{s_1} &= \hat{h_1}^* r(t) - \hat{h_2} r^*(t+T) \\ \hat{s_2} &= \hat{h_2}^* r(t) - \hat{h_2} r^*(t+T). \end{aligned} \tag{2.5}$$

In other words, estimated $\tilde{\mathbf{H}} = \left[\tilde{h_1}\ \tilde{h_2} \right]$ of $\mathbf{H}$ is necessary to accurately extract $\hat{\mathbf{S}} = \left[\hat{s_1}\ \hat{s_2} \right]$. That is even though CSIT is removed, the receiver in STBC conventionally requires channel state information (CSI) for assisting its demodulation, which can be obtained in a training

period before the symbol transmission. Assuming $\tilde{\mathbf{H}}$ is perfectly obtained and equalized into

$$\hat{\mathbf{H}} = \begin{bmatrix} \tilde{h_1}^* & -\tilde{h_2} \\ \tilde{h_2}^* & -\tilde{h_1} \end{bmatrix}, \tag{2.6}$$

the ML estimated $\mathbf{S}$ can be written as

$$\hat{\mathbf{S}} = \arg\min_{\mathbf{S} \in S} \{ \| \mathbf{R} - \hat{\mathbf{H}}\mathbf{S} \|_2^{\,2} \}, \tag{2.7}$$

where S is a matrix of entire possible symbols, and $\|\cdot\|_2$ represents Euclidean distance.

Because the Alamouti scheme is limited to a system with $n = 2$ transmit antennas, [43] has applied the theory of complex orthogonal design to enable orthogonal codes for systems with $n > 2$. Nevertheless, [5] and the references therein have proven that the orthogonal property of the codes in a system with $n > 2$ can be maintained, but with expenses of symbol and block length, which in turn makes code rate of the system drops. Moreover, there is no other schemes than the Alamouti's that achieves full code rate of 1, and the code rate of a system with $n > 2$ never exceeds 3/4. Fig. 2.9 shows the increased symbols length and block length, while the code rate continuously drops, of the complex orthogonal designs for systems with $2 \leq n \leq 18$. In sum, preservation of the orthogonal property of the codes in a system with $n > 2$ transmit antennas causes high complexity and sacrifices real-time capability.

Even though equipping many antennas on a transmitter might be considered as impractical due to the transmitter's limited space, applying STBC for a system with multiple transmitters is operable, especially in cooperative communication in WSN. The scheme is called distributed STBC (DSTBC) [7, 44]. Fig. 2.10 shows an example of cooperative communication system in WSN, relay cooperative transmission, where a relay (R) is responsible for maintaining the communication links between source (S) and destination (D) [6].

In a WSN employing DSTBC, a node will act as a relay if it successfully receives a packet from the source. The relays, then, generate a signature vector. The transmitted signals from the relays consist of both symbols s_1 and s_2, which are a product of identical encoded symbol matrix $\mathbf{S}$ and their unique signature vectors. Assuming $n = 2$ STBC codes are employed (Alamouti scheme), transmitted symbols of n_t^{th} participating relays, where $n_t \in N$ total number of nodes in the network, is

	Symbols k	Block Length p	Rate k/p
$n = 2$	2	2	1
$n = 3$	3	4	3/4
$n = 4$	6	8	3/4
$n = 5$	10	15	2/3
$n = 6$	20	30	2/3
$n = 7$	35	56	5/8
$n = 8$	70	112	5/8
$n = 9$	126	210	3/5
$n = 10$	252	420	3/5
$n = 11$	462	792	7/12
$n = 12$	924	1584	7/12
$n = 13$	1716	3003	4/7
$n = 14$	3432	6006	4/7
$n = 15$	6435	11440	9/16
$n = 16$	12870	22880	9/16
$n = 17$	24310	43758	5/9
$n = 18$	48620	87516	5/9

Fig. 2.9 Symbol length, block length, and code rate for $2 \leq n \leq 18$ complex orthogonal design [5].

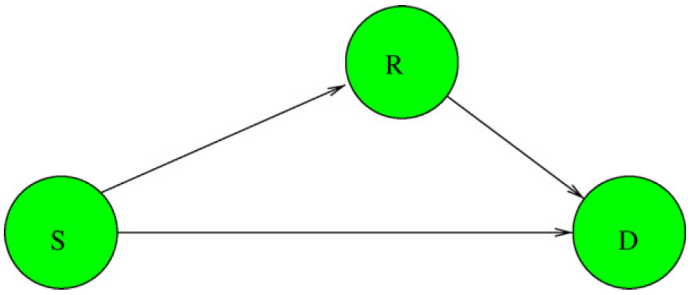

Fig. 2.10 An overview of relay cooperative transmission [6].

$$\mathbf{S}^{n_t} = \begin{bmatrix} w_{n_t,1} & w_{n_t,2} \end{bmatrix} \begin{bmatrix} s_1 & -s_2{}^* \\ s_2 & s_1{}^* \end{bmatrix} = W_{n_t}\mathbf{S}, \tag{2.8}$$

where W_{n_t} is a signature vector that is unique for each relay, Consequently, transmitted symbols at time t and $t+T$ are,

$$\begin{aligned} s^{n_t}(t) &= w_{n_t,1}s_1 + w_{n_t,2}s_2 \\ s^{n_t}(t+T) &= -w_{n_t,1}s_2{}^* + w_{n_t,2}s_1{}^*. \end{aligned} \tag{2.9}$$

W_{n_t} can be generated by optimization [44] or randomization [7]. The joint optimization scheme, however, is unattainable when a set of relays is undeterminded. Hence, the

randomization scheme overcomes the limitation by allowing each relay to independently generate its own W_{n_t}. A matrix containing W_{n_t} of entire participating relays N_t, thus, is

$$\mathbf{W} = \sqrt{\frac{1}{N_t}} \begin{bmatrix} \exp(j2\pi X_{1,1}) & \exp(j2\pi X_{1,2}) \\ \vdots & \vdots \\ \exp(j2\pi X_{n_t,1}) & \exp(j2\pi X_{n_t,2}) \\ \vdots & \vdots \\ \exp(j2\pi X_{N_t,1}) & \exp(j2\pi X_{N_t,2}) \end{bmatrix}, \tag{2.10}$$

where $X_{n_t,1}$ and $X_{n_t,2}$, $n_t \in N_t$, are uniformed distributed random variables within $[0, 1)$.

From Equation 2.9, n_t^{th} participating relay jointly transmits both symbols, s_1 and s_2, at the same time but with different ratio according to its w_{n_t}. By doing so, a distribution loss L_s occurs. According to [44], L_s of a DSTBC system with $n = 2$ (Alamouti scheme), is

$$L_s = 10log_{10}\left(\frac{1}{\frac{2}{N_t}\det\{\mathbf{W}^H\mathbf{W}\}^{1/2}}\right) \quad \text{dB}. \tag{2.11}$$

Equation 2.11 implies that more participating relays N_t induces more distribution loss L_s. A distribution loss L_s of the randomization scheme [7] with $\mathbf{W}$ in Equation 2.10 is also demonstrated in Fig. 2.11.

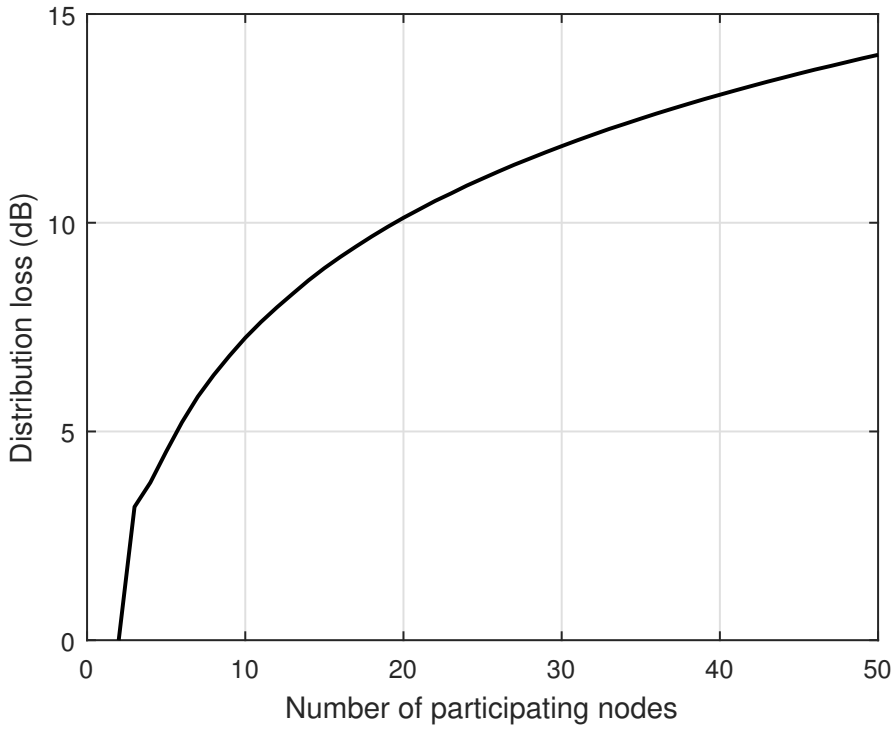

Fig. 2.11 Distribution loss L_s of the randomization scheme [7].

Chapter 3

Dumb spatial diversity techniques

A factory can be considered as a large indoor area, in which to cover the entire area, number of distributed transmitters should be massive, e.g., several tens to a hundred. Therefore, the techniques for achieving spatial diversity in previous works revealed in Chapter 2 cannot be applied straightforwardly because 1) the carrier frequency control in simulcast becomes excessively complicated, and 2) the randomization of unique signature vectors generates excessive distribution loss, while the acquisition of CSI also causes excessive latency. This chapter proposes to *dumb* the spatial diversity techniques in Chapter 2, in order to realize industrial wireless communication, where a massive number of transmitters is expected to be deployed. Before introducing the techniques, inevitable side effects from deploying the massive number of transmitters are first discussed. Thereafter, massive simultaneous transmission and massive simultaneous space-time block transmission are introduced. Investigations on the inevitable issues in each technique are also provided.

3.1 Side effects from massive transmission

In a system with a massive number of transmitters, uncertainties of individual transmitter result in severely transmission offsets. This section provides overviews of the offsets: carrier frequency offset (CFO) and timing offset (TO)

(a) Carrier frequency offset

The difference between carrier frequency that each transmitter uses to transmit the identical baseband signals refer to CFO. CFO is a result from instability of an oscillator in an individual transmitter. The instability varies with surrounding environment, such as temperature, and is limited within a range specified by a specification of the radio module. For example, CC2420 IEEE 802.15.4 standard compliant radio modules are allowed to have a frequency deviation f_D of $\pm 40ppm$ [45]. In other words, exact carrier frequency can be any value fell in a range of 2.45GHz±96kHz. Hence, phase cancellation of the simultaneous transmitted signals is unavoidable, and beats certainly occur. Fig. 3.1 demonstrates a combination of a hundred of identical signals with various CFO (red line) compared to an original signal (blue dot line), where the amplitude of the combined signal apparently changes.

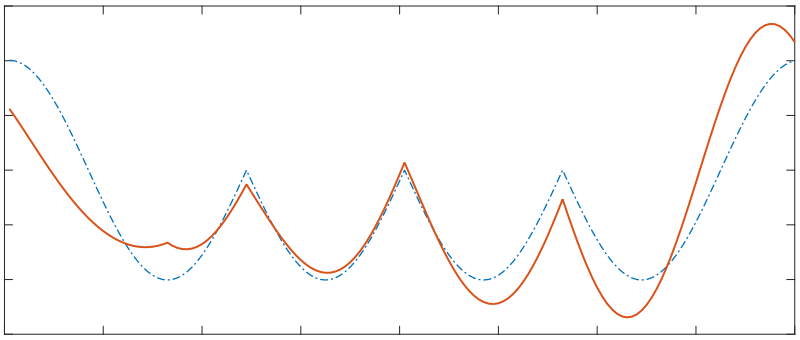

Fig. 3.1 Effect of carrier frequency offset on a combined signal.

(b) Timing offset

In addition to the instability of the oscillators, misalignment of an individual transmitter's internal clocks between the radio module and its microcontroller unit also results in individual transmission delay. The transmission delay pluses traveling time from the individual transmitter to a receiver causes the signals to arrive at the receiver at different time, and, hence, TO occurs. The total delay τ_e of a signal consists of software delay τ_{sw}, radio processing delay τ_d, packet transmission delay τ_{tx}, and propagation delay τ_p [4, 34]. Definitions of each delay are provided as follows:

- Software delay τ_{sw}: In a transmitter, the clocks of the microcontroller unit and the radio module can be unsynchronized. Due to this unsynchronization, τ_{sw} occurs during the signal transfer between these two components. Its value is shown to be a discrete random variable with granularity $1/f_r$, where f_r represents the radio clock frequency sourced by a crystal oscillator in a radio module.
- Radio processing delay τ_d: An individual transmitter occupies variable time for processing the incoming packet before starting the transmission. The processing time depends on the magnitude of the unsynchronized clocks between the control unit and the individual transmitter. The τ_d is shown to be a random variable with uniform distribution in the interval $[0, f_r]$.
- Packet transmission delay τ_{tx}: A drifted f_r, ρ, results in variable packet transmission time, hence, τ_{tx} occurs. The uncertainty of f_r can be caused by temperature and aging effects. τ_{tx} is shown to be approximately ρT_{slot}, T_{slot} is ideal packet transmission time.

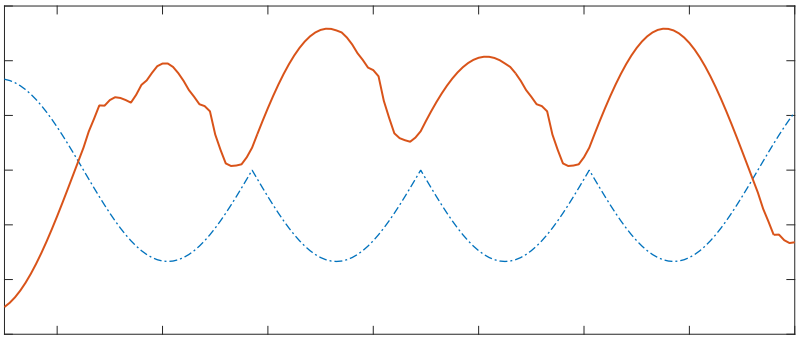

Fig. 3.2 Effect of timing offset on a combined signal.

- Propagation delay τ_p: τ_p depends on the distance d between individual transmitter and a receiver. Generally, $\tau_p = d/c$, where c is the velocity of light or approximately 3×10^{-8} m/s.

Hence, τ_e of individual transmitter is

$$\tau_e = \tau_{sw} + \tau_d + \tau_{tx} + \tau_p. \tag{3.1}$$

Fig. 3.2 demonstrates a combination of a hundred of identical signals with various delays, where phase of the combined signal (red line) changes and is obviously different from the original signal (blue dot line).

3.2 Massive simultaneous transmission

3.2.1 Overview

Although the simulcast is naturally capable for low latency, using simulcast in industrial wireless communication is excessively complicated due to the offset control of a massive number of transmitters. We propose massive simultaneous transmission, which inherits real-time capability from simulcast and simply achieves reliability and coverage by exploiting the diverse carrier frequencies of a massive number of transmitters, for industrial wireless communication.

An advantageous of massive simultaneous transmission over the conventional simulcast is that transmitter deployment is very simple. Because the succeed of conventional simulcast depends on CFO, which must be tightly set or ensured to be sufficient large, carefully

selecting transmitters to jointly perform simulcast is certainly essential. However, the selection becomes extremely complicated and impractical in a factory, where tens to a hundred of transmitters are expected to be distributed. To eliminate such the complication, massive simultaneous transmission allows a random deployment of the massive number of transmitters, where the selection of transmitters having relevant offsets are unnecessary.

3.2.2 Offset investigation

In the previous works of conventional simulcast, effects of CFO and TO including criteria for successful reception have been analyzed in a system with a few transmitters, i.e., less than ten, performing simulcast in one hop. However, a massive number of transmitters is crucial for industrial wireless communication in order to also achieve coverage area. Hence, to realize an effective massive simultaneous transmission, the effects of CFO and TO on the system are investigated as follows:

(a) CFO

The CFO control for successful reception in the previous works becomes irrelevant in massive simultaneous transmission. A combination of a massive number of simultaneously transmitted identical signals on slightly different carrier frequencies but synchronized time results in faster and narrower beats. Consequently, null points, where the amplitude of the signal severely drops, are reduced. In addition to the faster and narrower beats, erroneous demodulation is also reduced due to a protection from direct sequence spread spectrum (DSSS) employed in IEEE 802.15.4 standard and an increased SNR. That is, errors in chip level do not defect a bit demodulation because of the spread spectrum, and deploying a massive number of transmitters also raises the signal power. Therefore, CFO resulted from the nature of the radio modules does not disturb but even assists the demodulation in massive simultaneous transmission.

(b) TO

In contrast to CFO, TO is harmful in massive simultaneous transmission due to a severe ISI. A combination of a massive number of simultaneously transmitted identical signals with various delays results in excessive signal levels at a decision point, hence, it perturbs the receiver from correct demodulation. Therefore, the criteria of negligible ISI, consecutive arriving time of less than T_c in IEEE 802.15.4 standard compliant systems,

Table 3.1 Transmitted symbol sequences of massive simultaneous space-time block transmission.

	t	$t+T$
$s^{n_t,odd}$	s_1	$-{s_2}^*$
$s^{n_t,even}$	s_2	${s_1}^*$

in previous works does not hold any longer. An allowed delay for successful reception in massive simultaneous transmission, where a number of transmitted signals can be tens to hundred, becomes more strict.

3.3 Massive simultaneous space-time block transmission

3.3.1 Overview

In order to reduce the distribution loss L_s including the complexity of the randomization scheme [7] due to the distribution of the orthogonal codes to every transmitters, we propose massive simultaneous space-time block transmission. Massive simultaneous space-time block transmission employs Alamouti scheme, the only STBC scheme that achieves code rate of 1 for preserving the real-time capability of the system, and deterministically assigns each transmitter to permanently transmit either of the two encoded symbols. The transmitters are, as evenly as possible, divided into two groups according to their numbers, i.e., odd group and even group. The odd group is responsible for transmitting the first row of Equation 2.2, while the even group is responsible for transmitting the second row. At a time, transmitters in each group perform simultaneous transmission of an identical symbol. The sequences of symbol transmission of massive simultaneous space-time block transmission are shown in Table 3.1. By evenly dividing the transmitters into two groups, the distribution loss can be reduced because the randomized signature vectors that make the entire transmitters partially transmit either s_1 or s_2 is ensured to never occur.

The acquisition of CSI in conventional STBC including the randomization scheme [7] sacrifices the real-time capability of the system due to the training period before data transmission [29, 46–48]. In massive simultaneous space-time block transmission, an ML decoder where CSI is not required for demodulation [49] is thus employed, that is,

$$\hat{\mathbf{S}} = \arg\max_{\mathbf{S}\in S} \|\mathbf{S}\mathbf{R}^T\|. \tag{3.2}$$

Equation 3.2 can be seen as a matched filter. In order to identify $\mathbf{S}$ to match with the received signals $\mathbf{R}^T$, the number of DSSS chips in $\mathbf{S}$ should be at least 32, or a DSSS symbol. This is because non-coherent demodulation loses a degree of freedom of phase information, which is important in minimum shift keying (MSK) mod/demodulation. Fig. 3.3 illustrates autocorrelation of $\mathbf{S}$ with different numbers of chips, 2, 4, 8, 16, and 32, in a DSSS symbol. For distinguishing a symbol, using 32-chip $\mathbf{S}$ is capable to give a peak value, while the other numbers of chips fail to achieve autocorrelation of 1. Table 3.2 lists a relationship of data bits and chip sequences $\mathbf{S}$ for demodulation in massive simultaneous space-time block transmission.

3.3.2 Offset investigation

Receiver architecture of massive simultaneous space-time block transmission trades its complexity for the elimination of CSI, i.e., matched filter is employed. Therefore, the effects of CFO and TO resulted from simultaneous symbol transmission in each group can be investigated as follows:

(a) CFO

Fig. 3.4 demonstrates the autocorrelation of DSSS symbols in IEEE 802.15.4 standard compliant systems operating on 2.45GHz band with various CFO. It is obvious that, the signal remains itself only without CFO. With CFO, the signal loses its identity, and the larger the CFO, the less the signal be like an original one. Therefore, the CFO is harmful for massive simultaneous space-time block transmission.

(b) TO

Limited TO is not harmful to massive simultaneous space-time block transmission because the matched filter allows signals arriving at a receiver to have some delays. Because of its linear property, the matched filter can lock to a signal with least delay, so that there is a high possibility of correct demodulation if the locked signal arrives within an allowed delay, which ISI is still negligible. The autocorrelation of 4 DSSS symbols with an appearance of various timing offsets are shown in Fig. 3.5 as examples. It is obvious that, massive simultaneous space-time block transmission with a limited TO still yields high autocorrelation.

Table 3.2 S of massive simultaneous space-time block transmission.

Data bit	**S**
0 0 0 0	1 1 0 1 1 0 0 1 1 1 0 0 0 0 1 1 0 1 0 1 0 0 1 0 0 0 1 0 1 1 1 0
0 0 0 1	1 1 1 0 1 1 0 1 1 0 0 1 1 1 0 0 0 0 1 1 0 1 0 1 0 0 1 0 0 0 1 0
0 0 1 0	0 0 1 0 1 1 1 0 1 1 0 1 1 0 0 1 1 1 0 0 0 0 1 1 0 1 0 1 0 0 1 0
0 0 1 1	0 0 1 0 0 0 1 0 1 1 1 0 1 1 0 1 1 0 0 1 1 1 0 0 0 0 1 1 0 1 0 1
0 1 0 0	0 1 0 1 0 0 1 0 0 0 1 0 1 1 1 0 1 1 0 1 1 0 0 1 1 1 0 0 0 0 1 1
0 1 0 1	0 0 1 1 0 1 0 1 0 0 1 0 0 0 1 0 1 1 1 0 1 1 0 1 1 0 0 1 1 1 0 0
0 1 1 0	1 1 0 0 0 0 1 1 0 1 0 1 0 0 1 0 0 0 1 0 1 1 1 0 1 1 0 1 1 0 0 1
0 1 1 1	1 0 0 1 1 1 0 0 0 0 1 1 0 1 0 1 0 0 1 0 0 0 1 0 1 1 1 0 1 1 0 1
1 0 0 0	1 0 0 0 1 1 0 0 1 0 0 1 0 1 1 0 0 0 0 0 0 1 1 1 0 1 1 1 1 0 1 1
1 0 0 1	1 0 1 1 1 0 0 0 1 1 0 0 1 0 0 1 0 1 1 0 0 0 0 0 0 0 1 1 1 0 1 1 1
1 0 1 0	0 1 1 1 1 0 1 1 1 0 0 0 1 1 0 0 1 0 0 1 0 1 1 0 0 0 0 0 0 0 1 1 1
1 0 1 1	0 1 1 1 0 1 1 1 1 0 1 1 1 0 0 0 1 1 0 0 1 0 0 1 0 1 1 0 0 0 0 0
1 1 0 0	0 0 0 0 0 1 1 1 0 1 1 1 1 0 1 1 1 0 0 0 1 1 0 0 1 0 0 1 0 1 1 0
1 1 0 1	0 1 1 0 0 0 0 0 0 1 1 1 0 1 1 1 1 0 1 1 1 0 0 0 1 1 0 0 1 0 0 1
1 1 1 0	1 0 0 1 0 1 1 0 0 0 0 0 0 1 1 1 0 1 1 1 1 0 1 1 1 0 0 0 1 1 0 0
1 1 1 1	1 1 0 0 1 0 0 1 0 1 1 0 0 0 0 0 0 1 1 1 0 1 1 1 1 0 1 1 1 0 0 0

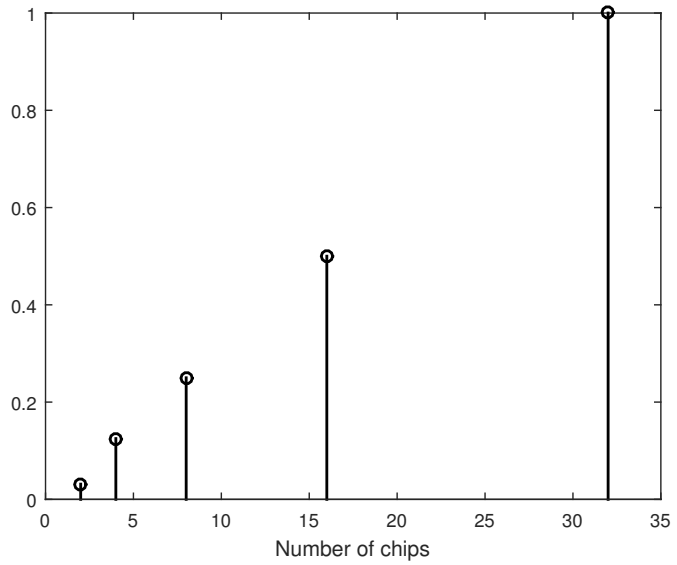

Fig. 3.3 Autocorrelation of various numbers of DSSS chips for demodulation in massive simultaneous space-time block transmission.

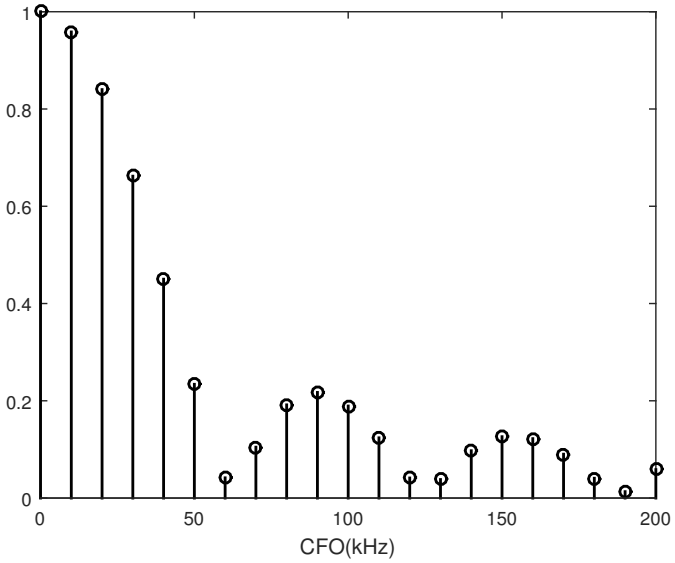

Fig. 3.4 Autocorrelation of DSSS symbols with various carrier frequency offsets.

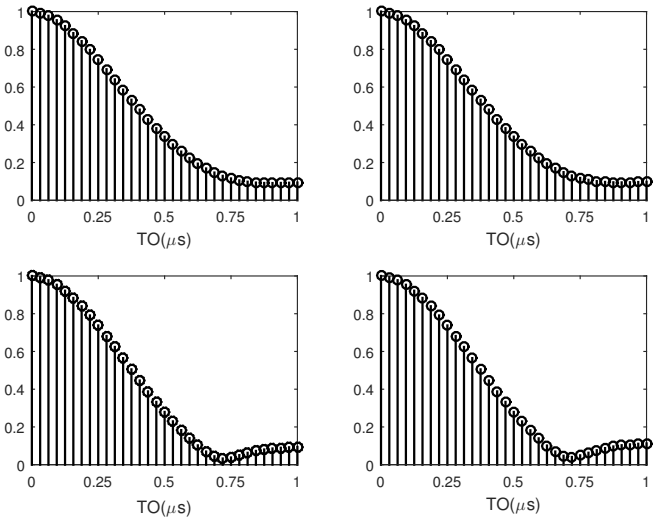

Fig. 3.5 Autocorrelation of DSSS symbols with various timing offsets.

Chapter 4

Evaluation

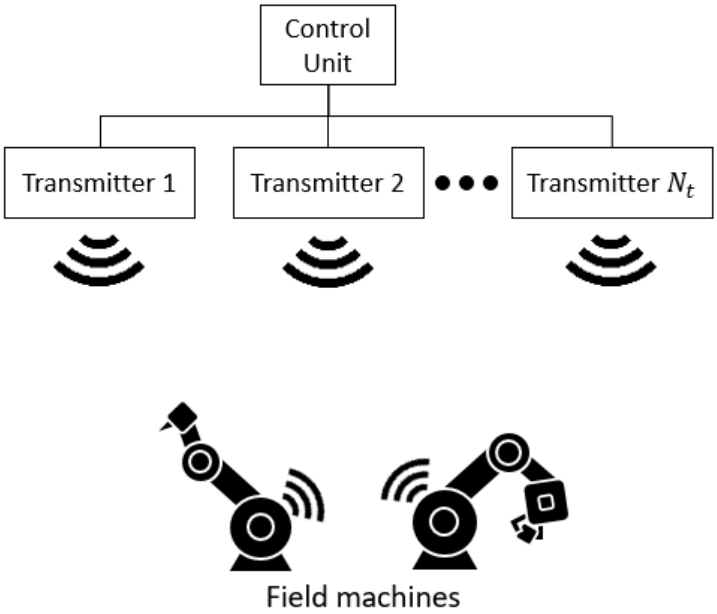

Fig. 4.1 An overview of dumb spatial diversity technique in a factory.

This chapter evaluates performances of the dumb spatial diversity techniques: massive simultaneous transmission and massive simultaneous space-time block transmission in a real factory environment by simulation in MATLAB. An overview of the wireless communication in a factory is shown in Fig. 4.1. The communication standard for the evaluation is IEEE 802.15.4 standard operating on 2.45GHz band [41], which is a promising standard for industrial wireless communication. The performances of the proposed schemes are evaluated by measuring their packet error rate (PER) when the number of transmitters is increased. Besides the simulation, experiments of massive simultaneous transmission on the IEEE 802.15.4 compliant devices are specially conducted in an indoor area with up to 32 transmitters. The simulation model and settings are first provided. The evaluated performances of each techniques are discussed afterward.

4.1 Simulation setup

In the simulation, a real factory with various transmission-offset scenarios are created. The identical signals are transmitted with equal power and arrive at a receiver with different attenuations, carrier frequencies, times, and phases. Placement of the transmitters and receivers, channel gain, the CFO, the TO, and the phases of each arriving signal are modeled as follows:

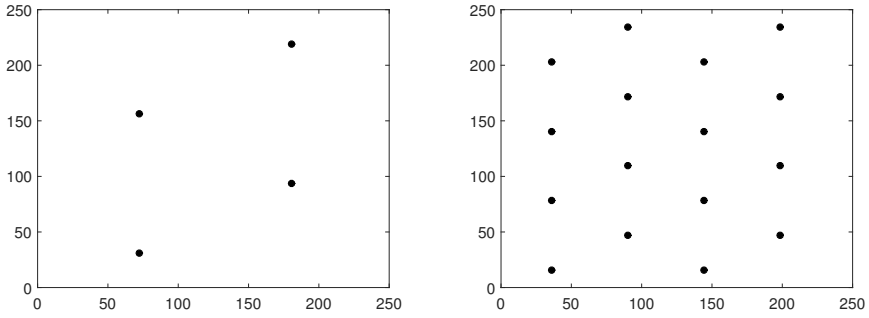

(a) 4 transmitters. (b) 16 transmitters.

Fig. 4.2 Transmitter placement in the simulation.

(a) Transmitter and receiver placement

The transmitters are assumed to be distributed on the ceiling of a factory in order to not only achieve coverage, but also increase SNR. The transmitters are placed in hexagonal cell plan, similar to base station placement in mobile communication. Fig. 4.2 illustrates transmitter placement in a factory with 4 and 16 transmitters as examples. The machines are assumed to be everywhere on the floor with 9 representing grid positions. Height of the factory is 4 meters in order to realize a real factory. Assuming x and y are coordinate positions of any transmitter or receiver in a two-dimension plane of a factory, distance d between a transmitter and a receiver, thus, is

$$d = \sqrt{(x_t^2 - x_r^2) + (y_t^2 - y_r^2) + 16}, \tag{4.1}$$

where the distance d is in a unit of meter, $\cdot_t$ refers to transmitter, and $\cdot_r$ refers to receiver.

(b) Channel gain

The channel gain in the simulation is calculated from path loss and shadowing in a factory. It demonstrates signal strength at a receiver after being attenuated. To obtain the channel gain, the channel attenuation of a factory with large-scale fading is first determined. Based on the comprehensive measurements in [50], the channel attenuation can be expressed as a summation of the path loss and the shadowing.

- Path loss: the path loss between n_t^{th} transmitter to a recevier can be calculated by

$$PL(d_{n_t}) = PL(d_0) + 10\nu \cdot \log(\frac{d_{n_t}}{d_0}), \tag{4.2}$$

  where $PL(d_0)$ is the path loss, in dB, at an arbitrarily chosen reference distance d_0 in meters, and ν is a path loss exponent.

- Shadowing: The shadowing is modeled as a lognormal distribution with 0 dB mean and a standard deviation σ.

Hence, the channel gain of a signal from n_t^{th} transmitter, G_{n_t}, is

$$G_{n_t} = P_t - (PL(d_{n_t}) + \text{Shadowing}), \tag{4.3}$$

where $n_t^{th} \in N_t$ total number of transmitters, and P_t represents transmit power in dB.

The signal that arrives at a receiver with the highest channel gain G_1 is defined as a reference signal. In massive simultaneous transmission, the carrier frequency, delay, and phase are f_1, τ_1, and ϕ_1, respectively. In massive simultaneous space-time block transmission, the carrier frequencies, delays, and phases are $f_{1,odd}$ and $f_{1,even}$, $\tau_{1,odd}$ and $\tau_{1,even}$, and $\phi_{1,odd}$ and $\phi_{1,even}$, respectively.

(c) CFO

The carrier frequencies of the transmitters can be deviated from the center frequency with the maximum value of f_D according to a specification in a standard. In the simulation, the arriving signals at a receiver are modeled to have their frequencies that offset from the reference signal. Hence, the CFO of the signal from n_t^{th} transmitters in massive simultaneous transmission is

$$\Delta f_{n_t} = f_1 - f_{n_t}, \tag{4.4}$$

and the CFO of the signal in massive simultaneous space-time block transmission can be either

$$\begin{aligned} \Delta f_{n_t,odd} &= f_{1,odd} - f_{n_t,odd}, \quad \text{or} \\ \Delta f_{n_t,even} &= f_{1,even} - f_{n_t,even}. \end{aligned} \tag{4.5}$$

The f_1, f_{n_t}, $f_{1,odd}$, $f_{n_t,odd}$, $f_{1,even}$, and $f_{n_t,even}$ are modeled to be normally distributed within $\pm f_D$ with standard deviation σ_f.

(d) TO

The total delay τ_e in Equation 3.1 of each arriving signal can be different due to the individual internal processes, thus, TO occurs. Similar to CFO, the τ_e of n_t^{th} transmitter is modeled referring to the reference signal. That is in massive simultaneous transmission,

$$\Delta\tau_{e,n_t} = \tau_1 - \tau_{e,n_t}, \tag{4.6}$$

and τ_e in massive simultaneous space-time block transmission can be either is

$$\begin{aligned} \Delta\tau_{e,n_t,odd} &= \tau_{1,odd} - \tau_{e,n_t,odd}, \quad \text{or} \\ \Delta\tau_{e,n_t,even} &= \tau_{1,even} - \tau_{e,n_t,even}. \end{aligned} \tag{4.7}$$

Consequently, the maximum TO among N_t transmitters can be expressed as

$$\delta = \max(\tau_1 - \tau_{e,n_t}) = \Delta \max(\tau_{e,n_t}), \tag{4.8}$$

for massive simultaneous transmission, and either

$$\begin{aligned} \delta &= \max(\tau_{1,odd} - \tau_{e,n_t,odd}) = \max(\Delta\tau_{e,n_t,odd}), \quad \text{or} \\ \delta &= \max(\tau_{1,even} - \tau_{e,n_t,even}) = \max(\Delta\tau_{e,n_t,even}), \end{aligned} \tag{4.9}$$

for massive simultaneous space-time block transmission. In the simulation, the $\Delta\tau_{e,n_t}$, $\Delta\tau_{e,n_t,odd}$, and $\Delta\tau_{e,n_t,even}$ are modeled to be uniformly distributed within the interval of $[-\frac{\delta}{2}, \frac{\delta}{2}]$.

(e) Phase

Phases of the signals are unequal due to the different carrier frequencies and the channels during the packet traveling. Hence, the arriving signal from n_t^{th} transmitters in massive simultaneous transmission are modeled to have a phase that offsets from the reference signal, that is

$$\Delta\phi_{n_t} = \phi_1 - \phi_{n_t}. \tag{4.10}$$

For massive simultaneous space-time block transmission, phases of the incoming signals are not referred to the reference signal. The arriving signals in the odd group have phases of $\{\phi_{1,odd}, \cdots, \phi_{n_t,odd}, \cdots\}$, and the even group have phases of $\{\phi_{1,even}, \cdots, \phi_{n_t,even}, \cdots\}$. In the simulation, ϕ_1, ϕ_{n_t}, $\phi_{1,odd}$, $\phi_{n_t,odd}$, $\phi_{1,even}$, and $\phi_{n_t,even}$ are set to fall randomly in $[0, 2\pi]$ in every packet.

In sum, system models of massive simultaneous transmission and massive simultaneous space-time block transmission are illustrated in Fig. 4.3 and Fig. 4.4, respectively. In addition, simulation and factory channel parameters including their values are shown in Table 4.1.

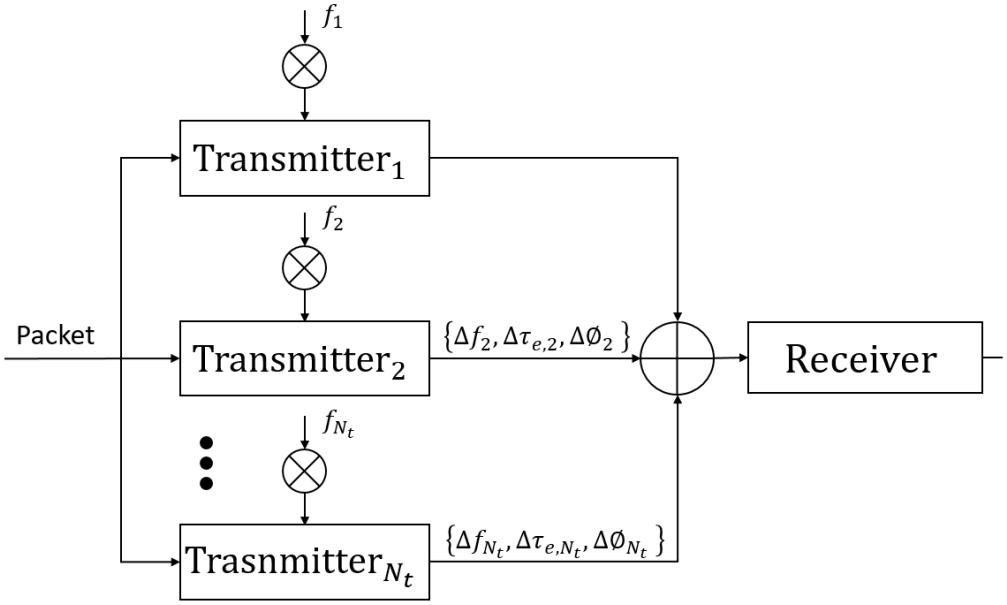

Fig. 4.3 System model of massive simultaneous transmission.

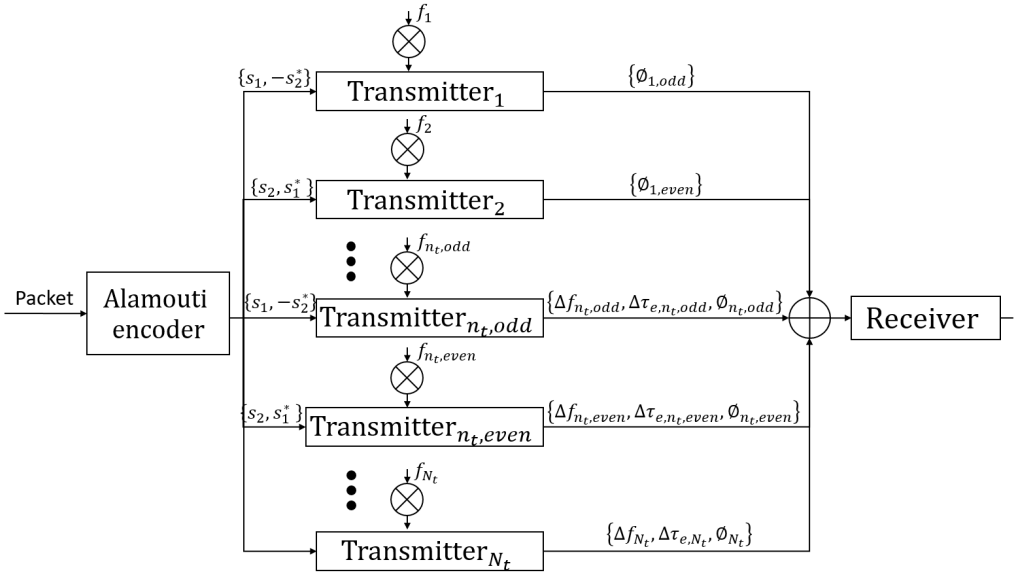

Fig. 4.4 System model of massive simultaneous space-time block transmission.

Table 4.1 Simulation parameters and factory channel settings.

Parameter	**Value**
Factory size	250m×250m
Transmit power (P_t)	0 dB
AWGN noise floor	-85 dBm
Path loss at a reference distance ($PL(d_0)$)	71.84 dB
Path loss exponent (ν)	2.16
Standard deviation of shadowing (σ)	8.13
Chip period (T_c)	0.5μs
Center frequency (f_c)	2.45 GHz
Maximum deviated frequency (f_D)	±40ppm or ±96kHz
Standard deviation of carrier frequency (σ_f)	$0, \frac{f_D}{2}, \frac{f_D}{3}, \frac{f_D}{5}$
Maximum timing offset (δ)	$0, \frac{T_c}{2}, T_c$
Packet length	20 bytes
Total number of packets	10,000
PER threshold for excellent performance	10^{-3}

4.2 Massive simultaneous transmission

4.2.1 Simulation results and discussions

Fig. 4.5 demonstrates the PER resulted from CFO with various standard deviation σ_f of massive simultaneous transmission, where the timing is synchronized. It is obvious that the appearance of CFO is preferred in massive simultaneous transmission as the PER is lower than that of the non-CFO scenario. In addition, the CFO criteria is also conforming to the previous work [3], that is the larger CFO yields better performance.

According to a measurement of carrier frequencies of 80 on-chip IEEE 802.15.4 standard compliant TelosB nodes in our laboratory, the standard deviation σ_f if found to be $\frac{f_D}{2}$ or 19.2 kHz. Therefore, $\sigma_f = \frac{f_D}{2}$ is set in hereafter simulation of massive simultaneous transmission to investigate the effect of TO.

Fig.4.6 demonstrates the PER of massive simultaneous transmission with various maximum TO, δ, where the increase of the number of transmitters causes PER floor when TO appears. The PER floor also depends on the δ, that is, larger δ results in higher PER floor. However, when the timing synchronization error does not appear, massive simultaneous

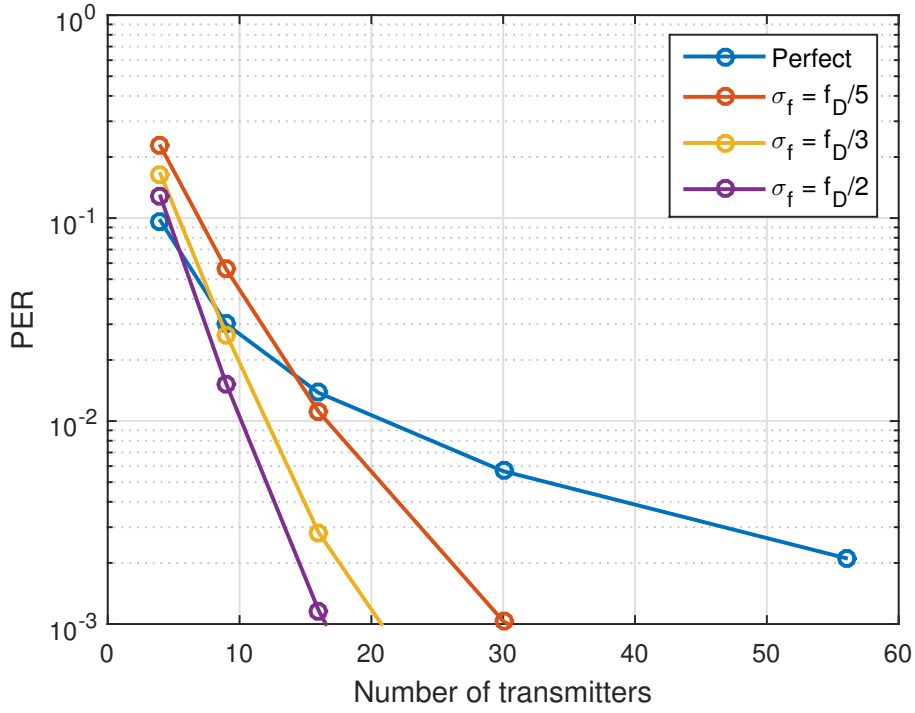

Fig. 4.5 The PER of massive simultaneous transmission in carrier frequency offset scenario.

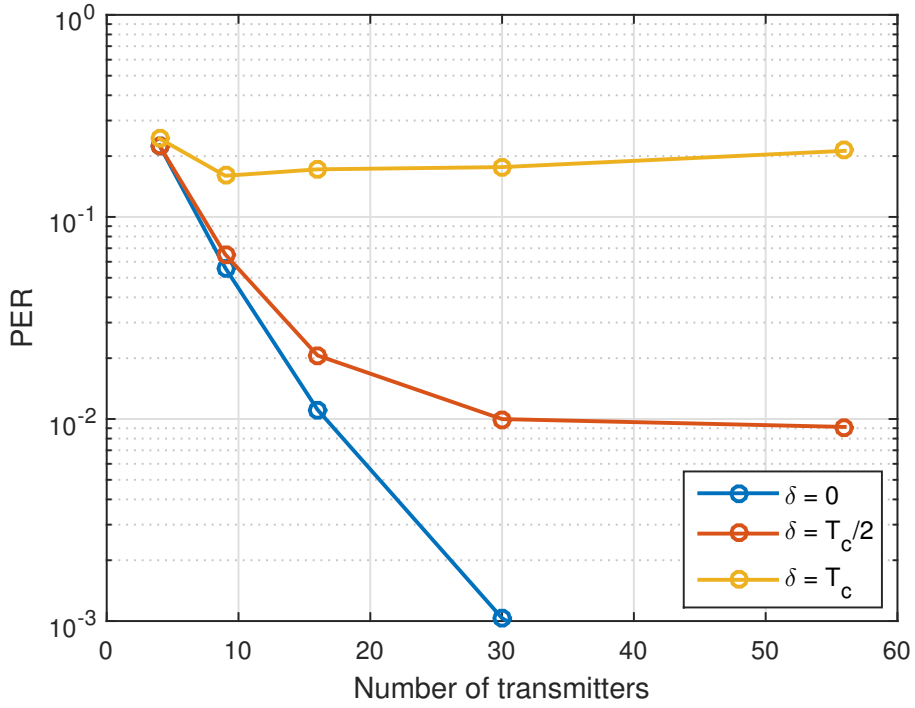

Fig. 4.6 The PER of massive simultaneous transmission in timing offset scenario.

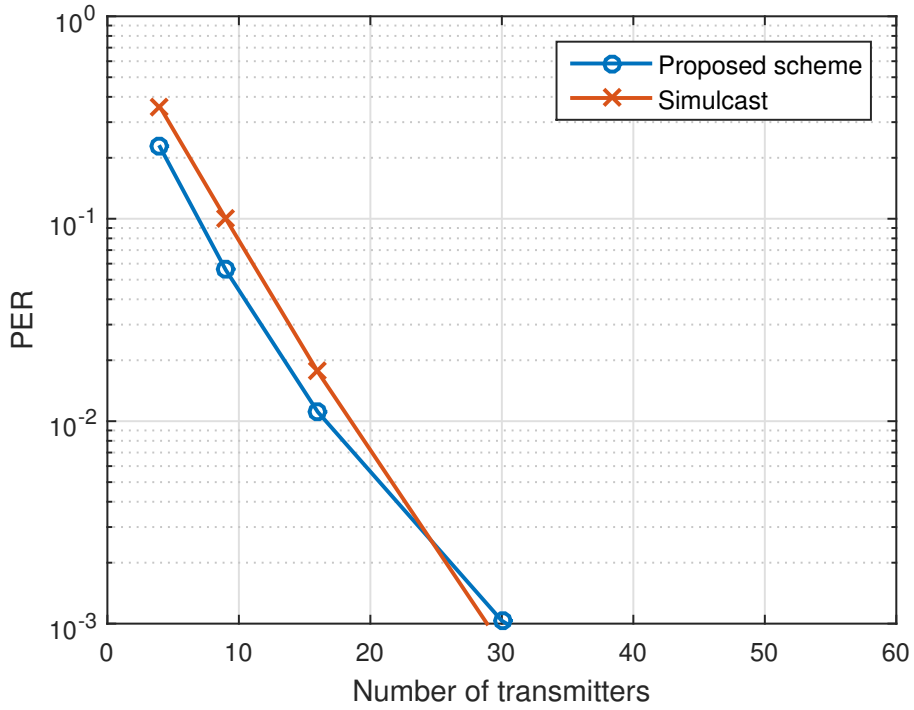

Fig. 4.7 The performance comparison of simulcast and massive simultaneous transmission.

transmission is able to yield an excellent performance if sufficient number of transmitters are deployed.

A comparison of the performances of massive simultaneous transmission and conventional simulcast is demonstrated in Fig. 4.7, where the blue line represents massive simultaneous transmission, and the red line represents conventional simulcast. The two schemes are compared under their effective scenario, i.e., perfect timing synchronization with an appearance of CFO. For the CFO control of conventional simulcast, the available interval of carrier frequency with maximum deviation is quantized into several steps. Those are, then, assigned to each transmitter to guarantee that the adjacent transmitters will have sufficient large CFO. According to the specification of CC2420 radio module [45], the carrier frequency interval is quantized into 7 steps, that is, CFO are {-96, -64, -32, 0, 32, 64, 96} kHz. Both massive simultaneous transmission and conventional simulcast yields similar performances. The PER decreases continuously as the number of transmitters increases. For example, PER of massive simultaneous transmission decreases from 0.226 to 0.011 at 4 and 16 transmitters, respectively. The massive simultaneous transmission, including conventional simulcast, provides an excellent performance when $N_t \geq 30$ transmitters are deployed as the achievable PER are below 10^{-3}. However, considering

deploying a massive number of transmitters in a factory for achieving coverage, massive simultaneous transmission provides considerably simpler transmitter deployment compared to the conventional simulcast.

4.2.2 Experiment

We specially conduct over-the-air experiments of the massive simultaneous transmission to investigate its feasibility in the real world.

(a) Setup

The Tmote Sky sensor nodes with TI CC2420 radio module (TelosB) [51] shown in Fig. 4.8 are deployed as the control unit, transmitters, and receivers, as they are compliant with the IEEE 802.15.4 standard and also cost efficient when deploying several tens of them. The experiments are conducted in an indoor area, where the layout is shown in Fig. 4.9. There are 3 groups of nodes: 1 initiator, up to 32 concurrent transmitters, and 8 receivers. The initiator acts as a control unit, which initiates packets to the transmitters and is placed at the center of a 7.6m×3.65m space and 1.4 m above the ground. The 4, 8, 16, 24, and 32 transmitters are grouped to perform each massive simultaneous transmission case. All the transmitters are randomly selected from total of 80 nodes in each round of the experiments and symmetrically placed on the two sides of a 2.2 m high wooden beam encircling the space. The receivers are placed 0.8 m above the ground to measure PER. The well-known timing synchronization protocol, namely Glossy [34], is applied to enable simultaneous transmission. The initiator transmits packets at 0 dBm to ensure each transmitter receives the packet before performing simultaneous transmission. Then, the transmitters simultaneously retransmit packets with -25 dBm to form the massive simultaneous transmission. We conduct 6 rounds of the experiments in which 1,000 packets are transmitted to each receiver in each round.

(b) Result

Fig. 4.10 shows the PER obtained and averaged over 6 rounds of the experiment. The PER slightly increases then becomes lower and saturated when the number of simultaneous transmitters is increased. The result also conforms with the simulation result in Fig. 4.6 at $\delta = T_c$. We compare the results at $\delta = T_c$ because 1) the possible δ in the experiments equals to 0.5 μs or T_c of the IEEE 802.15.4 standard since the TI CC2420 radio module has f_r of 8 MHz [45], and 2) τ_p in the experiments can be ignored due to the small area.

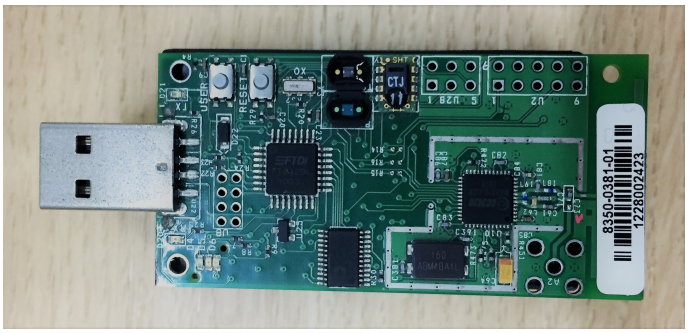

Fig. 4.8 Tmote Sky sensor node with TI CC2420 radio module (TelosB).

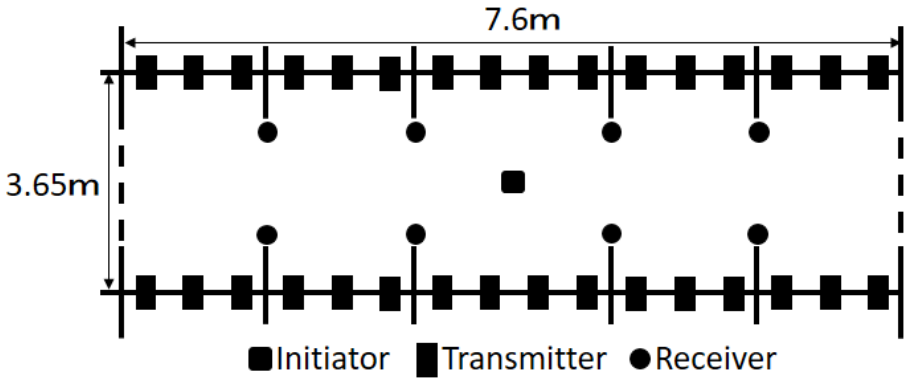

Fig. 4.9 Layout of the experiments.

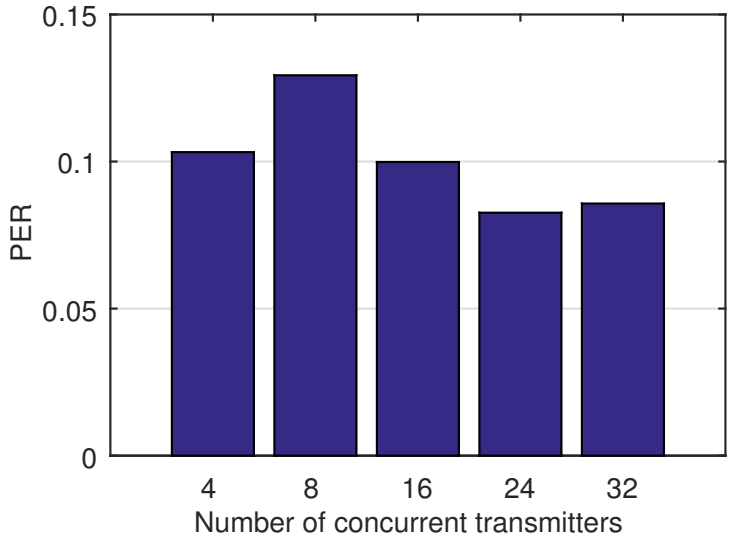

Fig. 4.10 The average PER obtained from the experiments.

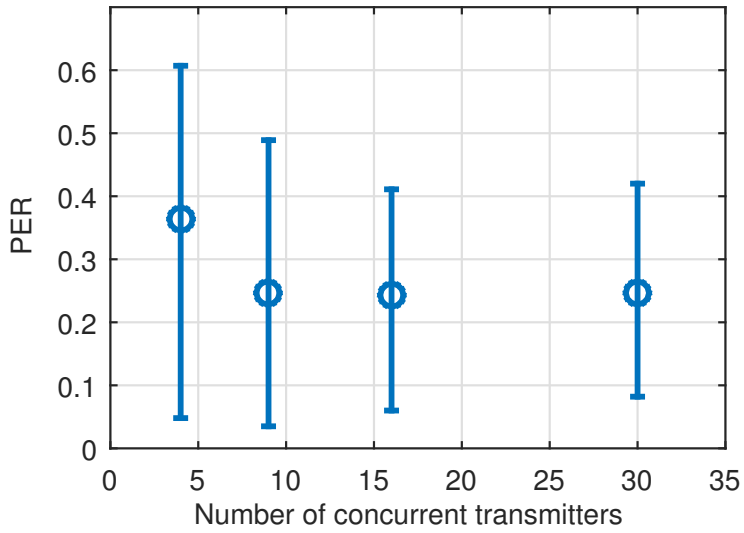

Fig. 4.11 The variation of PER at $\delta = T_c$ obtained by simulation.

Deploying 32 concurrent transmitters turns to be excessive as the PER floor of 0.08 occurs at 24 concurrent transmitters.

In addition, the variation of PER from the simulation with its maximum and minimum is shown in Fig. 4.11, where the setting is modified to realize the experimental environment. According to Fig. 4.11, it is possible that the PER of 4 concurrent transmitters is unexpectedly lower than that of 8 concurrent transmitters due to the limited number of rounds of the experiments. Note that, although the obtained PER in the experiments is insufficient for the high-reliability area criteria of 10^{-3}, it can be improved if the TO is reduced, for example, by increasing the f_r.

4.3 Massive simultaneous space-time block transmission

Fig. 4.12 demonstrates the PER of massive simultaneous space-time block transmission in a scenario where CFO appears but TO does not. It is obvious that, the appearance of the CFO is harmful to massive simultaneous space-time block transmission as the PER becomes worse when the number of transmitters is increased, regardless of small or large CFO.

In contrast to CFO, limited TO is not harmful to massive simultaneous space-time block transmission as demonstrated in Fig. 4.13. According to the receiver architecture,

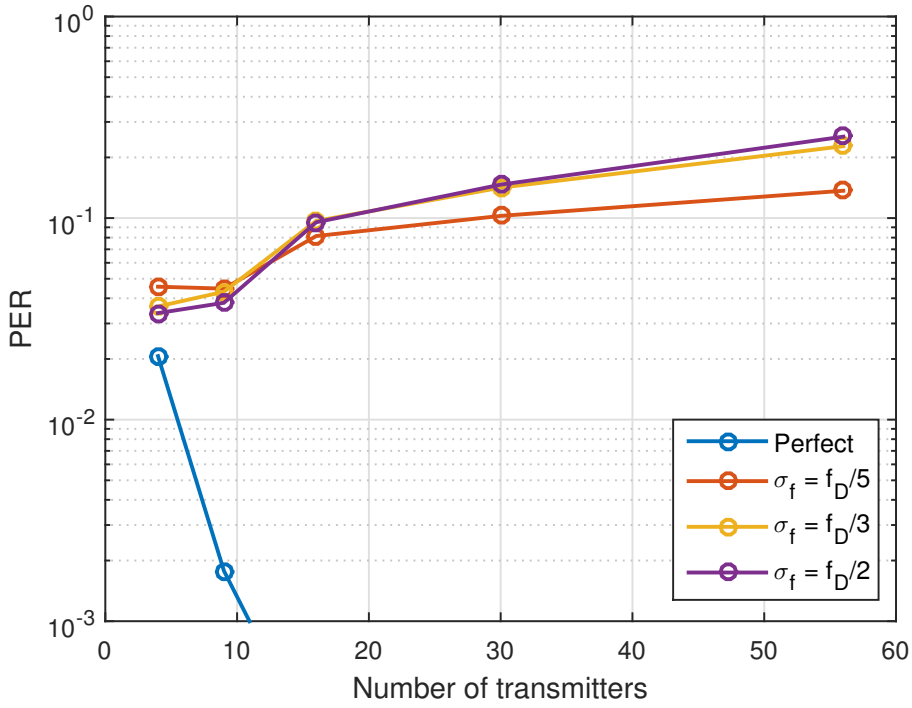

Fig. 4.12 The PER of massive simultaneous space-time block transmission in carrier frequency offset scenario.

the excellent performance is achievable even at $\delta = T_c/2$. Nevertheless, the performance is not improved when $\delta \geq T_c$, that is the ISI becomes excessively severe and disturb the demodulation. In addition, PER floor also occurs when the number of transmitters increases.

A comparison of the performances of massive simultaneous space-time block transmission (blue lines) and the DSTBC with randomized signature vector scheme [7] (red lines) under their best scenario: carrier frequency and timing are assumed to be synchronized, is demonstrated in Fig.4.14. The dot lines also show the PER of both schemes where CSI is used for demodulation at a receiver as references. Massive simultaneous space-time block transmission yields better performance compared to the DSTBC with randomized signature vector scheme [7]. PER of the massive simultaneous space-time block transmission decreases continuously when N_t is increased, from 0.021 at $N_t = 4$ to 0.002 at $N_t = 9$, and even become excellent at $N_t > 10$.

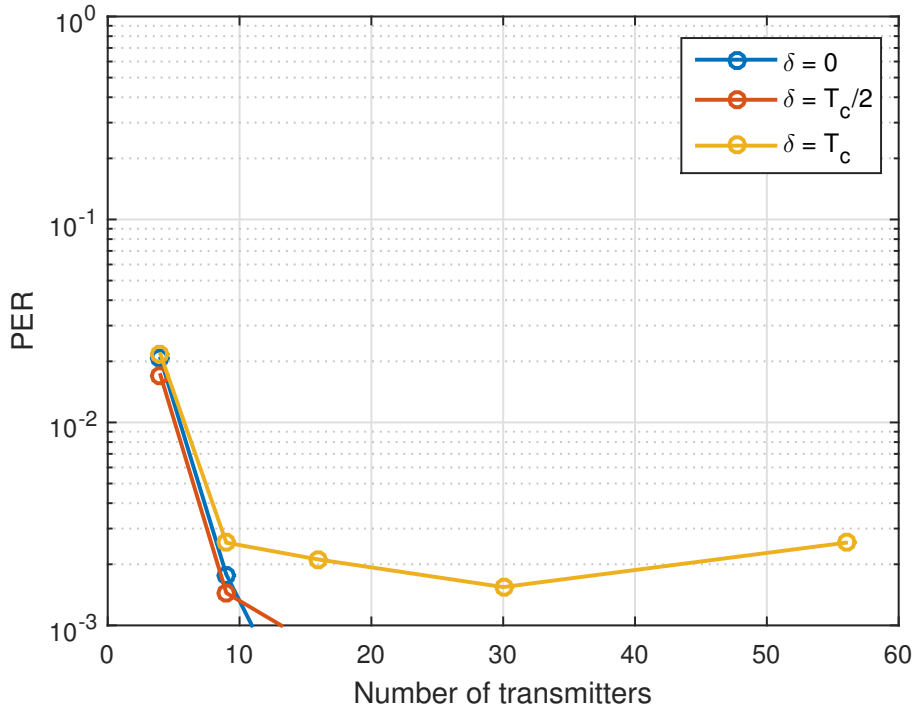

Fig. 4.13 The PER of massive simultaneous space-time block transmission in timing offset scenario.

4.4 Summary

In summary, massive simultaneous transmission and massive simultaneous space-time block transmission yields excellent performances when sufficient numbers of transmitters are deploy, i.e., several tens. Fig. 4.15 demonstrates the number of transmitters required to cover an entire factory area with high reliability under their best scenarios. The high-reliability area is defined as a location in which its PER is lower than 10^{-3}. In order to achieve 100% of the high-reliability area, massive simultaneous transmission and massive simultaneous space-time block transmission requires similar numbers of transmitters.

Nevertheless, both techniques are effective under different transmission-offset scenarios. Table 4.2 summarizes the recommended scenarios for each technique. The symbols ◯, △, and × represent performing 'best', 'moderately', and 'worst', respectively. Massive simultaneous transmission is recommended in a scenario where only CFO appears. On the other hands, massive simultaneous space-time block transmission is recommended in a scenario where carrier frequencies are synchronized, and, in addition, a limited TO can be allowed.

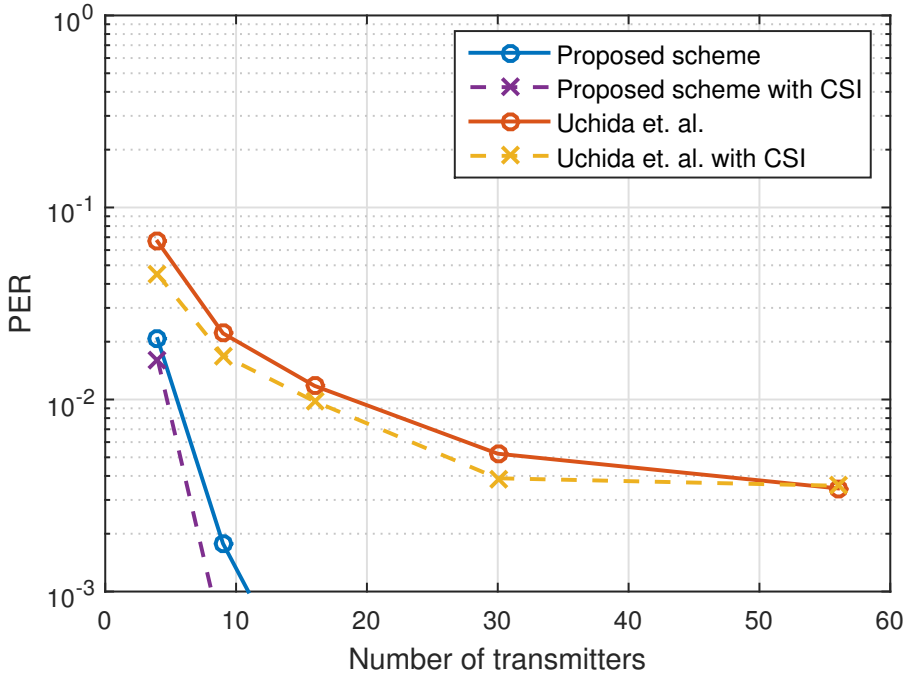

Fig. 4.14 The performance comparison of DSTBC with randomized signature vector scheme [7] and massive simultaneous space-time block transmission.

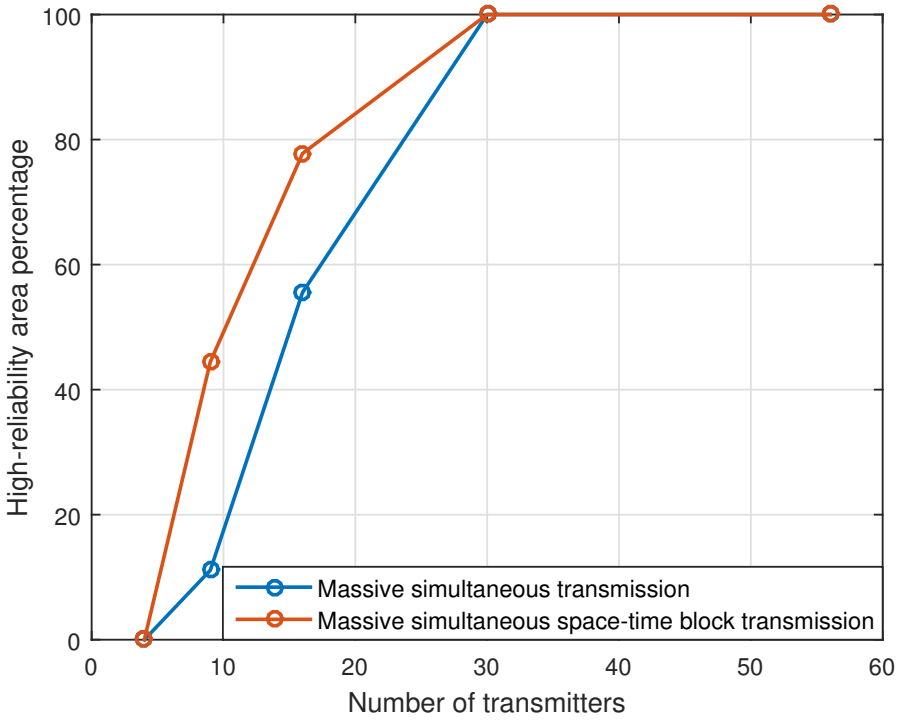

Fig. 4.15 The percentage of high-reliability area.

Table 4.2 The summary table of the offset scenarios for massive simultaneous transmission and massive simultaneous space-time block transmission.

	Synchronized scenarios		
	Timing and frequency	Timing (CFO appears)	Frequency (TO appears)
Massive simultaneous transmission	△	◯	×
Massive simultaneous space-time block transmission	◯	×	△ (limited TO)

Chapter 5

Conclusions and future works

This chapter concludes the works conducted in this thesis. Future works also are explained.

5.1 Conclusions

In order to enable a use of wireless links in industrial data communication, reliability and low latency of the system should be accomplished. This thesis proposes dumb spatial diversity techniques: massive simultaneous transmission and massive simultaneous space-time block transmission, for realizing industrial wireless communication. Open-loop spatial diversity techniques, simulcast and STBC, which are likely capable for low latency, are studied. However, in a factory, where a massive number of transmitters are expected to not only ensure the reliability, but also to achieve coverage area, the conventional spatial diversity techniques cannot be applied straightforwardly. Firstly, the carrier frequency control in simulcast becomes excessively complicated. Secondly, DSTBC, that makes STBC capable for multiple transmitters, induces excessive loss due to the code distribution over the transmitters, and the loss grows with the number of transmitters. Moreover, the acquisition of CSI for demodulation of the conventional STBC also induces additional latency.

On the other hand, massive simultaneous transmission inherits the real-time capability from simulcast, and, instead of controlling the CFO, exploits the advantageous fast fading-like phenomenon resulted from the randomness of carrier frequencies so that the transmitter deployment is very simple. Meanwhile, instead of sharing the orthogonal codes to every transmitters, massive simultaneous space-time block transmission deterministically assigns the codes to the transmitters to reduce the distribution loss. In addition, a ML demodulation where CSI is not required is also applied to enable the low latency.

The performances of the proposed techniques are evaluated in the simulation of a real factory environment with various transmission-offset scenarios: CFO and TO, where the communication are based on IEEE 802.15.4 standard operating on 2.45GHz band. The simulation results show that massive simultaneous transmission and massive simultaneous space-time block transmission yield excellent performances under different offset scenarios when sufficient numbers of transmitters are deployed. Massive simultaneous transmission is effective under an appearance of the CFO but disappearance of the TO. Massive simultaneous space-time block transmission, on the other hand, is effective under and a disappearance of the CFO but appearance of limited TO. The over-the-air experiments

of massive simultaneous transmission are specially conducted in order to investigate its feasibility in the real world. The experimental result also conforms with the simulation results. However, the performance in the real world is currently insufficient for the industrial wireless communication due to the hardware limitation of the on-chip devices.

5.2 Future works

The future works of this thesis include analysis of the distribution loss of massive simultaneous space-time block transmission and a relationship between required numbers of transmitters and a factory.

Firstly, since the distribution loss of massive simultaneous space-time block transmission cannot be calculated by using Equation 2.11, the loss resulted from simultaneous redundant symbol transmission should be analyzed in order to be able to clearly specify the performance of massive simultaneous space-time block transmission compared to the conventional STBC and DSTBC schemes.

Secondly, an equation represents a relationship between a factory and its required numbers of transmitters in order to achieve a 100% of high-reliability area will be derived to prevent an extravagant transmitter deployment.

Acknowledgments

First of all, I would like to express my deepest gratitude to my supervisor, Professor Hiroyuki Morikawa, for his guidance and endless supports on my studying throughout my master course including my research student period so that this thesis is properly accomplished. I also would like to appreciate guidance and helps from staffs in our laboratory, Project Researcher Makoto Suzuki and Research Associate Yoshiaki Narusue, who further advise me along my professor. In addition, I truly appreciate doctoral students in our laboratory, who always provide technical guidance, wireless communication knowledge, and research methodologies, Mr. Theerat Sakdejayont and Mr. Chun-Hao Liao. The thesis could not be accomplished without their helps and supports.

I deeply appreciate Ajinomoto Foundation for financial supporting throughout my master. I also would like to thank our members in the laboratory, who have been assisting and making me enjoy my life here. Finally, I would like to thank my family and friends who always support me in every possible ways.

Kulanuch Chutisemachai

August 2017

References

[1] A. Frotzscher, U. Wetzker, M. Bauer, M. Rentschler, M. Beyer, S. Elspass, and H. Klessig, "Requirements and current solutions of wireless communication in industrial automation," in *Proceedings of 2014 IEEE International Conference on Communications Workshops*, pp. 67–72, June 2014.

[2] T. Sexton, S. Souissi, and C. Hill, "Performance of high data rate paging in simulcast," in *Proceedings of 1997 Wireless Communications Conference*, pp. 43–49, August 1997.

[3] C. H. Liao, Y. Katsumata, M. Suzuki, and H. Morikawa, "Revisiting the so-called constructive interference in concurrent transmission," in *Proceedings of 2016 IEEE 41st Conference on Local Computer Networks*, pp. 280–288, November 2016.

[4] Y. Wang, Y. He, X. Mao, Y. Liu, Z. Huang, and X. Li, "Exploiting constructive interference for scalable flooding in wireless networks," in *Proceedings of 2012 IEEE International Conference on Computer Communications*, pp. 2104–2112, March 2012.

[5] W. Su, X.-G. Xia, and K. J. R. Liu, "A systematic design of high-rate complex orthogonal space-time block codes," *IEEE Communications Letters*, vol. 8, no. 6, pp. 380–382, June 2004.

[6] A. Willig, "How to exploit spatial diversity in wireless industrial networks," *Annual Reviews in Control*, vol. 32, no. 1, pp. 49 – 57, April 2008.

[7] R. Uchida, H. Okada, T. Yamazato, and M. Katayama, "Distributed space-time block coding for large and undetermined set of relay terminals," in *Proceedings of 2007 IEEE 18th International Symposium on Personal, Indoor and Mobile Radio Communications*, pp. 1–5, September 2007.

[8] V. N. Swamy, S. Suri, P. Rigge, M. Weiner, G. Ranade, A. Sahai, and B. Nikolic, "Cooperative communication for high-reliability low-latency wireless control," in *Proceedings of 2015 IEEE International Conference on Communications*, pp. 4380–4386, June 2015.

[9] G. Prytz, "A performance analysis of EtherCAT and PROFINET IRT," in *Proceedings of 2008 IEEE International Conference on Emerging Technologies and Factory Automation*, pp. 408–415, September 2008.

[10] J. D. Decotignie, "Ethernet-based real-time and industrial communications," *Proceedings of the IEEE*, vol. 93, no. 6, pp. 1102–1117, June 2005.

[11] T. Skeie, S. Johannessen, and O. Holmeide, "Timeliness of real-time IP communication in switched industrial Ethernet networks," *IEEE Transactions on Industrial Informatics*, vol. 2, no. 1, pp. 25–39, February 2006.

[12] J. d. Decotignie, "The many faces of industrial ethernet," *IEEE Industrial Electronics Magazine*, vol. 3, no. 1, pp. 8–19, March 2009.

[13] R. Drath and A. Horch, "Industrie 4.0: Hit or hype?" *IEEE Industrial Electronics Magazine*, vol. 8, no. 2, pp. 56–58, June 2014.

[14] M. Hermann, T. Pentek, and B. Otto, "Design principles for industrie 4.0 scenarios," in *Proceedings of 2016 49th Hawaii International Conference on System Sciences*, pp. 3928–3937, January 2016.

[15] J. Lee, B. Bagheri, and H.-A. Kao, "A cyber-physical systems architecture for industry 4.0-based manufacturing systems," *Manufacturing Letters*, vol. 3, pp. 18 – 23, January 2015.

[16] X. Li, D. Li, J. Wan, A. V. Vasilakos, C.-F. Lai, and S. Wang, "A review of industrial wireless networks in the context of industry 4.0," *Wireless Networks*, vol. 23, no. 1, pp. 23–41, January 2017.

[17] V. C. Gungor and G. P. Hancke, "Industrial wireless sensor networks: Challenges, design principles, and technical approaches," *IEEE Transactions on Industrial Electronics*, vol. 56, no. 10, pp. 4258–4265, Octotber 2009.

[18] P. Rawat, K. D. Singh, H. Chaouchi, and J. M. Bonnin, "Wireless sensor networks: A survey on recent developments and potential synergies," *The Journal of Supercomputing*, vol. 68, no. 1, pp. 1–48, April 2014.

[19] D. Dzung, C. Apneseth, J. Endresen, and J. E. Frey, "Design and implementation of a real-time wireless sensor/actuator communication system," in *Proceedings of 2005 IEEE Conference on Emerging Technologies and Factory Automation*, vol. 2, pp. 10 pp.–442, September 2005.

[20] J. Song, S. Han, A. Mok, D. Chen, M. Lucas, M. Nixon, and W. Pratt, "WirelessHART: Applying wireless technology in real-time industrial process control," in *Proceedings of 2008 IEEE Real-Time and Embedded Technology and Applications Symposium*, pp. 377–386, April 2008.

[21] T. Hasegawa, H. Hayashi, T. Kitai, and H. Sasajima, "Industrial wireless standardization - scope and implementation of ISA SP100 standard," in *Proceedings of 2011 Society of Instrument and Control Engineers Annual Conference*, pp. 2059–2064, September 2011.

[22] H.-C. Yang and M. S. Alouini, "Performance analysis of multibranch switched diversity systems," *IEEE Transactions on Communications*, vol. 51, no. 5, pp. 782–794, May 2003.

[23] A. Gorokhov, "Antenna selection algorithms for MEA transmission systems," in *Proceedings of 2002 IEEE International Conference on Acoustics, Speech, and Signal Processing*, vol. 3, pp. III–2857–III–2860, May 2002.

[24] M. Gharavi-Alkhansari and A. B. Gershman, "Fast antenna subset selection in wireless MIMO systems," in *Proceedings of 2003 IEEE International Conference on Acoustics, Speech, and Signal Processing*, vol. 5, pp. V–57–60 vol.5, April 2003.

[25] H. Zhang and H. Dai, "Fast transmit antenna selection algorithms for MIMO systems with fading correlation," in *Proceedings of 2004 IEEE 60th Vehicular Technology Conference*, vol. 3, pp. 1638–1642 Vol. 3, September 2004.

[26] T. Tang and R. W. Heath, "Opportunistic feedback for downlink multiuser diversity," *IEEE Communications Letters*, vol. 9, no. 10, pp. 948–950, October 2005.

[27] S. Jin, X. Li, and X. Gao, "Statistical transmit antenna selection for correlated rayleigh fading MIMO channels," in *Proceedings of 2006 IEEE 63rd Vehicular Technology Conference*, vol. 4, pp. 1665–1669, May 2006.

[28] B. Fang, Z. Qian, W. Shao, and W. Zhong, "RAISE: A new fast transmit antenna selection algorithm for massive MIMO systems," *Wireless Personal Communications*, vol. 80, no. 3, pp. 1147–1157, February 2015.

[29] C. Fragouli, N. Al-Dhahir, and W. Turin, "Training-based channel estimation for multiple-antenna broadband transmissions," *IEEE Transactions on Wireless Communications*, vol. 2, no. 2, pp. 384–391, March 2003.

[30] S. Joshi, "Effect of antenna spacing on the performance of multiple input multiple output LTE downlink in an urban microcell," *International Journal of Wireless & Mobile Networks*, vol. 4, pp. 175–188, December 2012.

[31] A. A. M. Saleh, A. Rustako, and R. Roman, "Distributed antennas for indoor radio communications," *IEEE Transactions on Communications*, vol. 35, no. 12, pp. 1245–1251, December 1987.

[32] P. Chow, A. Karim, V. Fung, and C. Dietrich, "Performance advantages of distributed antennas in indoor wireless communication systems," in *Proceedings of 1994 IEEE Vehicular Technology Conference*, pp. 1522–1526 vol.3, June 1994.

[33] J. Lu and K. Whitehouse, "Flash flooding: Exploiting the capture effect for rapid flooding in wireless sensor networks," in *Proceedings of 2009 IEEE International Conference on Computer Communications*, pp. 2491–2499, April 2009.

[34] F. Ferrari, M. Zimmerling, L. Thiele, and O. Saukh, "Efficient network flooding and time synchronization with Glossy," in *Proceedings of the 10th ACM/IEEE International Conference on Information Processing in Sensor Networks*, pp. 73–84, April 2011.

[35] D. Yuan and M. Hollick, "Let's talk together: Understanding concurrent transmission in wireless sensor networks," in *Proceedings of 38th Annual IEEE Conference on Local Computer Networks*, pp. 219–227, October 2013.

[36] M. Suzuki, Y. Yamashita, and H. Morikawa, "Low-power, end-to-end reliable collection using glossy for wireless sensor networks," in *Proceedings of 2013 IEEE 77th Vehicular Technology Conference*, pp. 1–5, June 2013.

[37] M. Wilhelm, V. Lenders, and J. B. Schmitt, "On the reception of concurrent transmissions in wireless sensor networks," *IEEE Transactions on Wireless Communications*, vol. 13, no. 12, pp. 6756–6767, December 2014.

[38] T. Hattori and K. Hirade, "Multitransmitter digital signal transmission by using offset frequency strategy in a land-mobile telephone system," *IEEE Transactions on Vehicular Technology*, vol. 27, no. 4, pp. 231–238, November 1978.

[39] S. Souissi, S. Sek, and H. Xie, "The effect of frequency offsets on the performance of FLEX(R) simulcast systems," in *Proceedings of 1999 IEEE 49th Vehicular Technology Conference*, vol. 3, pp. 2348–2352 vol.3, July 1999.

[40] T. Hattori, K. Hirade, and F. Adachi, "Theoretical studies of a simulcast digital radio paging system using a carrier frequency offset strategy," *IEEE Transactions on Vehicular Technology*, vol. 29, no. 1, pp. 87–95, February 1980.

[41] "IEEE standard for local and metropolitan area networks–part 15.4: Low-rate wireless personal area networks (LR-WPANs)," *IEEE Std 802.15.4-2011 (Revision of IEEE Std 802.15.4-2006)*, pp. 1–314, September 2011.

[42] S. M. Alamouti, "A simple transmit diversity technique for wireless communications," *IEEE Journal on Selected Areas in Communications*, vol. 16, no. 8, pp. 1451–1458, October 1998.

[43] V. Tarokh, H. Jafarkhani, and A. R. Calderbank, "Space-time block codes from orthogonal designs," *IEEE Transactions on Information Theory*, vol. 45, no. 5, pp. 1456–1467, September 2006.

[44] S. Yiu, R. Schober, and L. Lampe, "Distributed space-time block coding," *IEEE Transactions on Communications*, vol. 54, no. 7, pp. 1195–1206, July 2006.

[45] *CC2420 Datasheet*, Texas Instruments, 2007.

[46] T. L. Marzetta, "BLAST training: Estimating channel characteristics for high capacity space-time wireless," in *Proceedings of 37th Annual Allerton Conference on Communications, Control, and Computing*, pp. 958–966, 1999.

[47] M. Biguesh and A. B. Gershman, "Training-based MIMO channel estimation: a study of estimator tradeoffs and optimal training signals," *IEEE Transactions on Signal Processing*, vol. 54, no. 3, pp. 884–893, March 2006.

[48] F. Gao, T. Cui, and A. Nallanathan, "On channel estimation and optimal training design for amplify and forward relay networks," *IEEE Transactions on Wireless Communications*, vol. 7, no. 5, pp. 1907–1916, May 2008.

[49] M. Uysal and C. N. Georghiades, "An efficient implementation of a maximum-likelihood detector for space-time block coded systems," *IEEE Transactions on Communications*, vol. 51, no. 4, pp. 521–524, April 2003.

[50] E. Tanghe, W. Joseph, L. Verloock, L. Martens, H. Capoen, K. V. Herwegen, and W. Vantomme, "The industrial indoor channel: Large-scale and temporal fading at 900, 2400, and 5200 MHz," *IEEE Transactions on Wireless Communications*, vol. 7, no. 7, pp. 2740–2751, July 2008.

[51] *TelosB Datasheet*, Moteiv Corporation, May 2004.

Publications

国際会議

[1] K. Chutisemachai, T. Sakdejayong, C. H. Liao, M. Suzuki, and H. Morikawa “Distributed antenna system using concurrent transmission for wireless automation system,” To appear in Proceedings of the IEEE 86$^{\text{th}}$ Vehicular Technology Conference 2017, Toronto, Canada, Sep. 2017.

全国大会

[2] K. Chutiseamchai, T. Sakdejayont, C. H. Liao, M. Suzuki, and H. Morikawa, “Distributed antenna system using concurrent transmission with loose carrier frequency control in wireless factory,” 電子情報通信学会ソサイエティ大会，B-5-99，September 2016.

[3] K. Chutiseamchai, T. Sakdejayont, C. H. Liao, M. Suzuki, and H. Morikawa, “Feasibility of distributed antenna system using concurrent transmission in real world,” 電子情報通信学会総合大会，B-5-141，March 2017.